PHOTOCHEMISTRY OF 5*H*-DIBENZO[A,C]CYCLOHEPTENE

by

David Patrick Budac
B.Sc., University of Victoria, 1988

A Thesis Submitted in Partial Fulfillment of the
Requirements for the Degree of

MASTER OF SCIENCE

in the Department of Chemistry

We accept this thesis as conforming
to the required standard

[redacted]
Dr. P.C. Wan, Supervisor (Department of Chemistry)

[redacted]
Dr. A. Fischer, Departmental Member (Department of Chemistry)

[redacted]
Dr. R.D. Burke, Outside Member (Department of Biology)

[redacted]
Dr. Steven Holdcroft, External Examiner (Simon Fraser University)

Supervisor: Dr. P.C. Wan

Abstract

The photochemistry of 5*H*-dibenzo[a,c]cycloheptene (DAC) (**6**) has been studied in CH_3CN, aqueous CH_3CN and other organic solvents. The aim of the investigation was to determine whether this compound behaved as an ionizing carbon acid in S_1. It has already been reported, based on work done in this group, that a related compound, 5*H*-dibenzo[a,d]cycloheptene (DAD) (**1**), was a very strong carbon acid in S_1. Since **1** and a derivative were the only excited state carbon acids reported it was important to see whether **6** would exhibit similar behaviour.

Exchange of the methylene protons of DAC (**6**) with D_2O was observed on photolysis in D_2O–CH_3CN solution, under conditions where there was no exchange without irradiation. Quantum yields for deuterium incorporation in **6** have been measured. These results indicate that **6** is indeed an ionizing carbon acid in S_1.

In addition to carbon acid behaviour, a competing formal di-π-methane rearrangement to give dibenzonorcaradiene (DBN) (**50**) was observed in all solvents. In 100% CH_3CN, this rearrangement was the exclusive photochemical reaction. Detailed investigations of this formal di-π-methane rearrangement showed that two mechanisms were operative. In S_1 the rearrangement was via a 1,7-hydrogen shift followed by

electrocyclic ring closure. From T_1, a true di-π-methane mechanism operated. Quantum yields for the rearrangement have been measured in a variety of solvents.

The exchange process is believed to involve initial deprotonation of the methylene proton by the solvent as base (H_2O or D_2O), forming a carbanion, which is then protonated. The kinetics of the deprotonation step have been studied by fluorescence quenching and lifetime measurements.

Examiners:

[redacted]

Dr. P.C. Wan, Supervisor (Department of Chemistry)

[redacted]

Dr. A. Fischer, Departmental Member (Department of Chemistry)

[redacted]

Dr. R.D. Burke, Outside Member (Department of Biology)

[redacted]

Dr. Steven Holdcroft, External Examiner (Simon Fraser University)

TABLE OF CONTENTS

Preliminary Pages

Chapter One

Chapter 2 - Results and Discussion

Chapter Three - Experimental

List of Tables

List of Figures

ACKNOWLEDGEMENTS

I would like to express my appreciation to my supervisor, Dr. Peter Wan for his guidance and assistance throughout the past two years. As well I am grateful to him for providing me with the opportunity to travel and learn.

I would like to thank all those that have made my studies so enjoyable (at times) especially my friends Deepak Shukla and Erik Krogh.

I would also like to thank my family for their support especially my sister Lillian Budac for caring.

TO MY MOTHER

JOSEPHINE BUDAC

WHO PAST AWAY WHEN THIS WORK STARTED

CHAPTER 1

INTRODUCTION

Many of the concepts of reactivity and structure which apply for organic molecules in the ground state (S_o) do not apply for excited states. For example aromatic and antiaromatic species display chemistry in the excited state not observed in S_o[1,2].

The carbon acid behaviour of 5*H*-dibenzo[a,d]cycloheptene (DAD) (**1**) and fluorene (**2**) in the excited state provides an illustration of the variation in aromatic and antiaromatic character in the excited state[3]. DAD (**1**) exchanges its dibenzylic protons when irradiated in 50% D_2O-CH_3CN (eq. 1.1)[3]. Fluorene (**2**), which also has dibenzylic protons, does not exchange them when it is irradiated under the same conditions (eq. 1.2). In S_o, the pK_a of fluorene (**2**) (dibenzylic

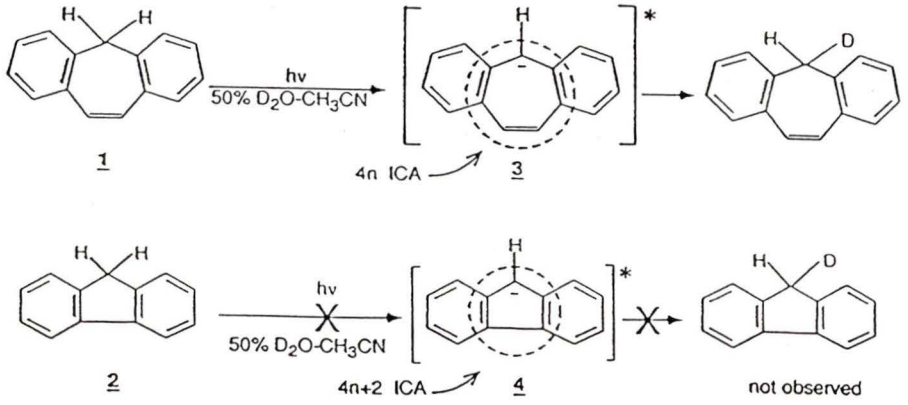

protons) is ≈22[4] while the same protons of DAD (**1**) are in the range of ≈32-36[5]. This difference in pK_a can be rationalized by looking at the carbanion intermediates formed upon

deprotonation of these two molecules. Ground state deprotonation of fluorene (**2**) leads to an aromatic 6π (4n+2) internal cyclic array (ICA), as in **4**, while deprotonation of DAD (**1**) gives an antiaromatic 8π (4n) ICA **3**. The fluorenyl anion (**4**) is relatively stable (i.e., aromatic) in S_o, in contrast to the dibenzo[a,c]cycloheptenyl anion (**3**), which is antiaromatic. The exchange process in the singlet excited state (S_1) is believed to go via these carbanion intermediates. Since DAD (**1**) exchanges its dibenzylic protons after excitation and fluorene (**2**) does not, the formally ground state antiaromatic intermediate **3** must be favoured in S_1. The reverse could be said for intermediate **4**.

Photolysis of 5*H*-dibenzo[a,d]cycloheptane (DADA) (**5**)[3], under the same conditions as above did not result in proton exchange. This result demonstrates the importance of the ICA in the proton exchange of DAD (**1**) since this system is not capable of forming an ICA upon deprotonation.

DAD (**1**) is the first reported example of an ionizing excited state carbon acid. An isomer of DAD (**1**), 5*H*-dibenzo-[a,c]cycloheptene (DAC) (**6**), will be shown to display similar photochemistry. The position of the benzene rings in DAC (**6**) may also permit a competing formal di-π-methane photorearrangement. The remainder of this Introduction will delineate the concepts of aromaticity, antiaromaticity and excited state proton transfer. Less emphasis will be placed on material concerning the formal di-π-methane

photorearrangement of DAC (**6**) as similar rearrangements are well documented in the literature.

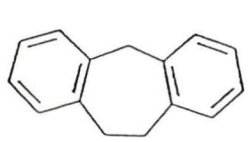

5

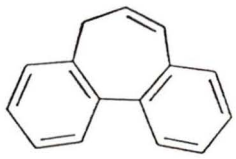

6

1.1 Excited State Acid-Base Chemistry

Acid-base chemistry is a fundamental process involved in many chemical and biological transformations. Factors which influence acid-base chemistry must be considered to completely understand these transformations. One important factor is the change observed in pK_a between the ground and excited states. The first person to start research in this area was Weber[6], who in 1931, observed a shift in the fluorescence spectrum of 1-naphthylamine-4-sulphonate (**7**) with a change in pH. In 1949 Förster[7] recognized these shifts as being due to excited state proton transfer (ESPT). Several years later Weller[8], a student of Förster, developed a method for relating the shift of the fluorescence spectrum to the excited state pK_a. Since that time extensive studies have continued on a variety of substituted aromatic compounds.

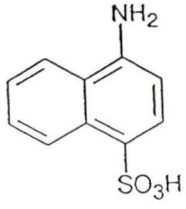

7

1.1.1 Stoke's Shift and ESPT

Fluorescence spectra can be shifted in wavelength when the excited molecule and/or its solvent shell rearrange[11]. These shifts are termed Stoke's shift and range in size depending on the extent of rearrangement. As noted by Weber[8], large Stoke's shifts occur in the fluorescence spectra of molecules which undergo ESPT. This shift is due to the formation of a *new emissive species* in the excited state by loss or gain of a proton. As the pH is changed, the fluorescence spectrum of the new species grows in. This is demonstrated by the fluorescence spectrum of 2-naphthol (**8**) at various pH (Fig. 1.1)[10].

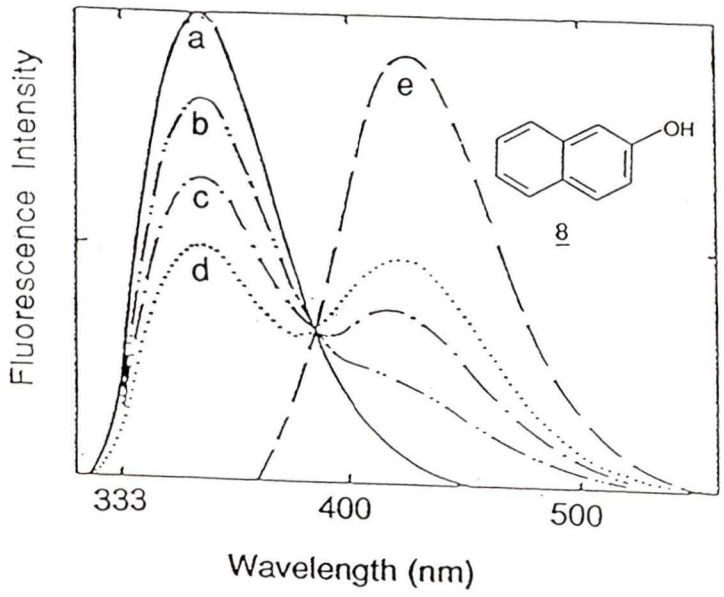

Figure 1.1 Stoke's shift in the fluorescence spectrum of 2-naphthol (**8**) with increasing pH a-e.

In general the fluorescence spectrum is shifted to longer

wavelengths (or to lower energies) when ESPT occurs. The shift can occur for deprotonation or protonation of a molecule. For aromatic molecules with electron withdrawing substituents such as carboxylates, carbonyls, and amides, protonation in the excited state shifts the fluorescence spectrum to longer wavelengths[11,12]. The fluorescence spectrum of aromatic molecules with electron donating substituents such as hydroxyls, amines and sulfhydryls, are also shifted to longer wavelengths but after deprotonation[11,12].

Electron withdrawing substituents are protonated (undergo a decrease in acidity) in the excited state[12] due to an increase in electron density on the substituent. Electron withdrawing substituents, of the type indicated (*vide supra*), have low lying π orbitals which can accept electrons from the π orbital of the aromatic ring when excitation occurs. A decrease in acidity is then seen for these substituents. The carboxyl substituent of benzoic acid (**9**) is an example which demonstrates these changes in the excited state (Scheme 1.1)[11,13].

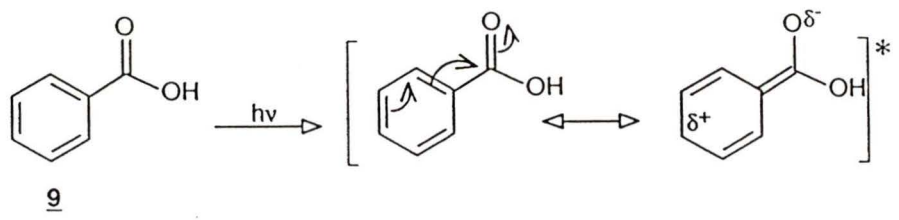

9

Scheme 1.1

The Stoke's shift observed for ESPT results from the

protonation of these electron rich substituent in the excited state[12]. Protonation in S_1 reduces the charge build up on the substituent making the protonated species ($^*BH^+$) more stable than the deprotonated species ($^*B$) (Fig. 1.2). In S_o the protonated species (BH^+) is less stable than the deprotonated (B), since the charge build up on the substituent is no longer present. Therefore the difference in energy between S_0 and S_1 of the protonated species ($\Delta E'$) is smaller than the energy difference between the same states of the deprotonated

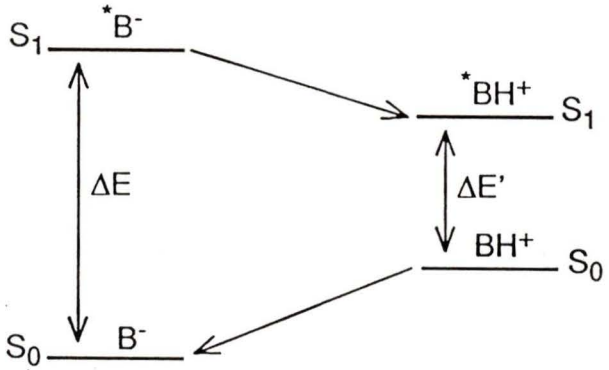

Figure 1.2 Reduction in energy gap for protonated electron withdrawing substituents leading to Stoke's shift.

species (ΔE). This reduction in the energy gap leads to a shift in the fluorescence spectrum to longer wavelengths (or to lower energies) similar to that seen in Figure 1.1.

For electron donating substituents, such as hydroxyls, amines and sulfhydryls, the opposite is true[12]. These substituents have lone pairs of electrons which can be donated

into the π system of the aromatic ring when excitation occurs. The hydroxyl substituent of phenol (**10**) provides an example which illustrates these changes in the excited state (Scheme 1.2)[11,13].

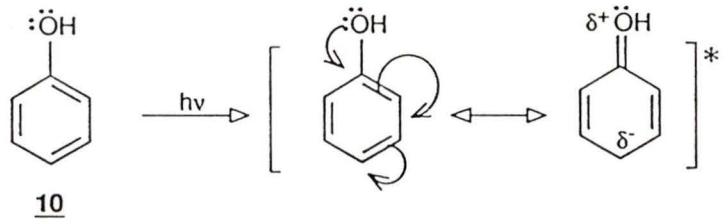

10

Scheme 1.2

Deprotonation of electron donating substituents is favoured in the excited state since the difference in energy ($\Delta E'$) between S_0 and S_1 of the deprotonated species (A^-, $^*A^-$) is smaller than the difference (ΔE) for the protonated species (HA, *HA) (Fig. 1.3). The fluorescence emission will therefore be shifted to longer wavelength (or lower energies) but for deprotonation[12].

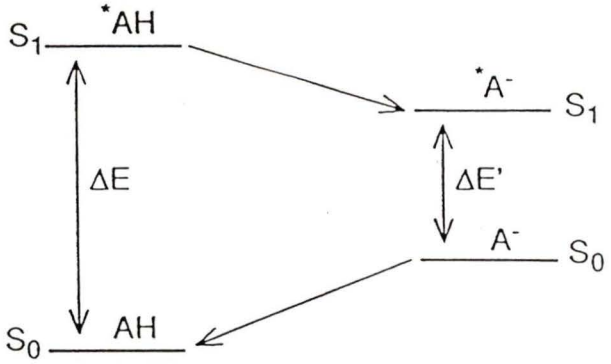

Figure 1.3 Reduction in the energy gap for deprotonated electron donating substituents leading to Stoke's shift.

1.1.2 Magnitude of pK_a Change in S_1 and T_1 Versus S_0

To date this Introduction has indicated that ESPT occurs in the singlet excited state (S_1). The triplet state (T_1) is also involved but higher order states such as S_2, S_3, etc. and T_2, T_3, etc. are not. This results from vibrational relaxation which competes effectively with ESPT, taking these higher energy states to S_1 and T_1 respectively[14].

The trends seen with different substituents in the previous section apply to both S_1 and T_1. However changes in pK_a involving T_1 are generally smaller than changes involving S_1[11]. Two types of structures which are believed to represent the molecules in S_1 and T_1 can be used to explain this difference[13].

The first is a charge transfer (C-T) resonance structure (Fig. 1.4)[13]. These C-T structures have an energy above that of S_1 (Fig.1.5). The proximity of S_1 and C-T may result in the mixing of these two levels. Molecules in S_1, can therefore be represented by the C-T structure. T_1 has an energy lower than S_1 and therefore cannot mix with the C-T level. Substituents of molecules in T_1 will therefore have less of a charge build up, than those in S_1. The change in pK_a between S_o and T_1 will in turn be smaller as the charge buildup dictates the extent to which the pK_a is altered[12].

A more important contributor to molecules in T_1 is a diradical species (Fig. 1.4)[13]. With the diradical species there is less of a charge build up on the substituents,

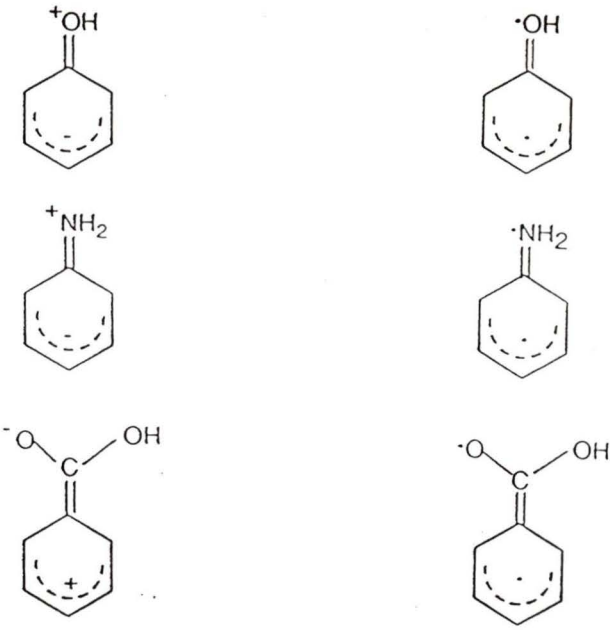

C-T Structures **Diradical Structures**

Figure 1.4 Contributors to S_1 (C-T structures) and T_1 (diradical structures).

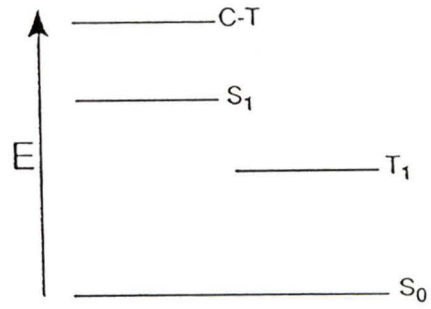

Figure 1.5 Location of the C-T energy level relative to the S_1 and T_1 energy levels.

compared to that shown for the substituents of the C-T structures. Therefore a smaller change will be observed in the pK_a after excitation to T_1.

1.1.3 Carbon Acids in the Excited State

The discussion of ESPT in the previous section dealt with changes in pK_a for oxygen, nitrogen and sulphur acids. No examples of carbon acids were presented because none have been observed (prior to studies by our group) to undergo proton exchange on excitation. Fluorene (**2**) has been predicted by Förster cycle calculations[12], to undergo a substantial increase in acidity on excitation (pK_a of 20.5 in S_0 to -8.5 in S_1)[11]. To date no experimental results have been obtained to indicate that this change in pK_a actually takes place. Such a change may be disallowed simply because insufficient time exists for the deprotonation of a carbon acid in the excited state. For example, in the ground state, the rate of deprotonation by ^-OH observed for fluorene (**2**) in H_2O is $\approx 10^4$ $M^{-1}s^{-1}$ [15]. Deactivational processes such as fluorescence and intersystem crossing are generally much faster ($\approx 10^8$ s^{-1}) [16]. Carbon acids are therefore returned to the ground state before deprotonation occurs. Proton transfer involving oxygen, nitrogen and sulphur can occur at the rate of diffusion (10^{10} $M^{-1}s^{-1}$)[17] and do compete with the deactivational processes.

Differences in the rates of deprotonation observed for carbon acids and oxygen, nitrogen and sulphur acids have been ascribed to the location of the lone pair of electrons after deprotonation[17]. The lone pair of electrons remain on the oxygen, nitrogen and sulphur when deprotonation occurs (eq. 1.3). With carbon, the lone pair is delocalized to adjacent

atoms to stabilize the anion formed (eq. 1.4). Along with this delocalization, rehybridization and rearrangements must occur. These changes involving carbon acids lead to rates of deprotonation which are much slower then rates observed for oxygen, nitrogen and sulphur acids.

$$ROH \xrightarrow{-H^+} RO^- \qquad (1.3)$$

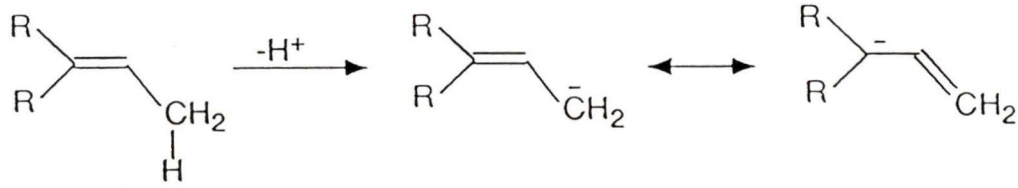

(1.4)

All carbon acids do not undergo rehybridization and rearrangements on deprotonation. Carbon acids which do not involve delocalization of the carbanion, are termed equilibrium carbon acids[4]. An example of such a carbon acid is phenylacetylene (**11**) (eq. 1.5)[17]. Carbon acids which do involve delocalization of the carbanion are termed kinetic acids[4].

$$PhC{\equiv}C{-}H \underset{}{\overset{-H^+}{\rightleftharpoons}} PhC{\equiv}C^- \qquad (1.5)$$

11

DAD (**1**) could be termed an excited state kinetic carbon acid if the anion **3** is stabilized by delocalization in an excited state such as S_1. The initial deprotonation to give

the carbanion could, however, be completed in S_1 (adiabatic) or start in S_1 with subsequent formation of the carbanion in S_o (diabatic) (Fig. 1.6)[16].

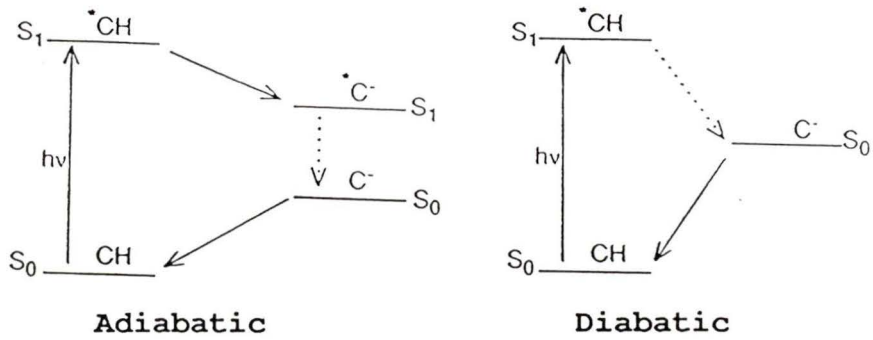

Figure 1.6 Adiabatic vs diabatic photochemical processes.

A diabatic process would occur if the S_o and S_1 potential energy surfaces of DAD (**1**) approached each other at some point (Fig. 1.7)[18]. This situation exists when the geometry of the excited molecule resembles a geometry in S_o[14]. At such points between the potential energy surfaces the molecule can be transferred from S_1 to S_o. It should be noted that the point of transfer shown is at the transition state for deprotonation leading to DAD^- (**3**). Therefore the diabatic process involves partial deprotonation of DAD (**1**) in the excited state. The molecule, at the top of the energy curve in S_o, can either return to its original form, before excitation, or go down the other side to form products. If the product produced is formed via an intermediate on the S_o surface then the photochemical reaction is termed a hot ground state reaction[14].

As shown by Figure 1.7 the photochemical proton exchange of DAD (**1**) could occur via such a process.

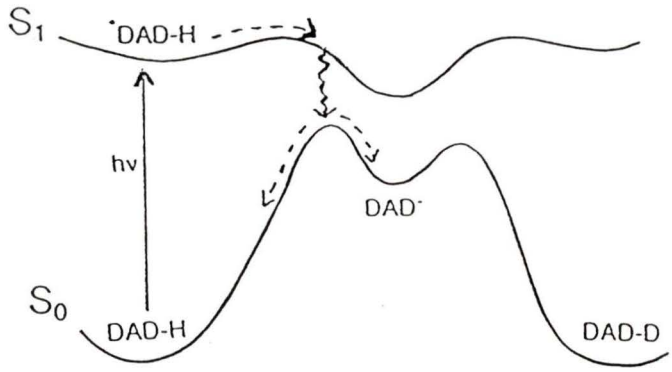

Figure 1.7 The potential energy surfaces involved in a diabatic photochemical process with DAD (**1**) as an example.

An adiabatic photochemical process is also possible (Fig. 1.8)[18]. Excitation of DAD (**1**) would place the molecule on the

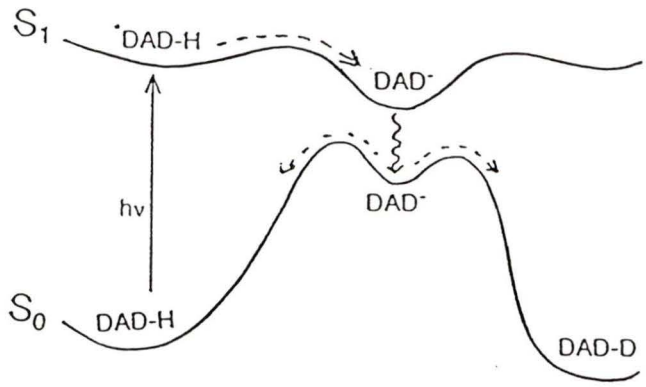

Figure 1.8 Potential energy surfaces required for an adiabatic photochemical process involving DAD (**1**)

S_1 potential energy surface where deprotonation would occur to give the excited state carbanion. The carbanion would then be transferred to the ground state surface where protonation or deuteration occurs.

No evidence exists to indicate which of these two possibilities, or variations of them, is occurring. However, the processes do indicate that partial deprotonation of DAD (**1**) may take place in the excited state. If this photochemical deprotonation was occurring for the reasons indicated for other ESPT processes, then a compound similar to DAD (**1**), fluorene (**2**) should exhibit the same behaviour. However, it was shown that **2** does not exchange its dibenzylic protons after irradiation in D_2O[3]. Another rational must be used to explain the contrasting photochemical behaviour of DAD (**1**) and fluorene (**2**).

1.2 Aromaticity and Antiaromaticity in the Excited State

Aromaticity, as defined by Hückel's rule, states that cyclic arrays of orbitals with 4n+2 π electrons (where n=0,1,2,...) have a special stability[19]. Benzene (**12**), demonstrates this concept since it contains a 6π (4n+2) cyclic array and is stable in S_o. Breslow[20] proposed that systems with 4n cyclic arrays of π electrons which are destabilized relative to acyclic analogs, be known as antiaromatic. Cyclobutadiene (**13**), with a 4π (4n) cyclic array, demonstrates this concept as it is less stable then 1,3-butadiene (**14**) in

S_o.

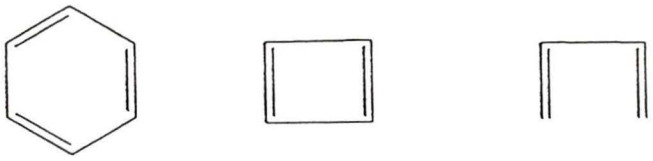

12 13 14

Ground state aromatic and antiaromatic species display chemistry in the excited state not observed in S_o. Examples are described in the following section.

1.2.1 The Behaviour of Aromatic and Antiaromatic Species in the Excited State

Benzene (**12**) and cyclobutadiene (**13**) are molecules which exhibit chemistry in the excited state not observed in S_o. As indicated earlier **12** is aromatic in S_o and is therefore inert under a variety of reaction conditions[21]. In the excited state, however, **12** exhibits a high degree of unimolecular reactivity (eq. 1.6)[22]. Cyclobutadiene (**13**) is antiaromatic

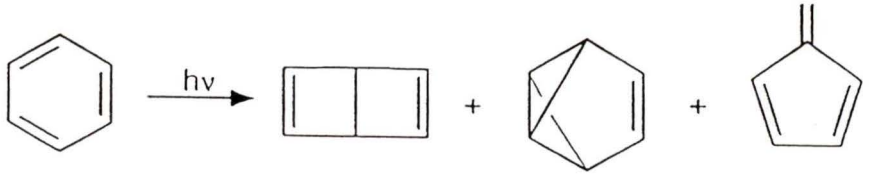

12 (1.6)

and reactive since it dimerizes in S_o (eq. 1.7)[22,23,24]. No dimerization is observed after extensive photolysis of **13**[1].

The structures of **12** and **13** are both altered in S_1. Theoretical calculations on the bond lengths of **12** and **13** in

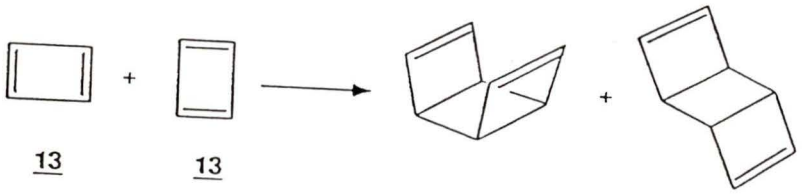

13 13 (1.7)

S_o and S_1 indicate this change[1]. In S_o **13** exists as a rectangular species[23,24,25] whereas in S_1 it takes on a square structure[1] (eq. 1.8). This indicates that the double bonds of

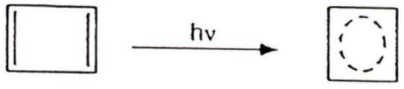

13 (1.8)

13 are delocalized in S_1. A comparison of the calculated bond lengths for benzene (**12**) in S_o and S_1 reveals that the delocalization observed in S_o is disrupted in S_1 since a symmetrical hexagonal structure no longer exists[1,26].

Results obtained by Wan and coworkers[27], provide further examples of aromatic and antiaromatic species which display chemistry in the excited state not observed in S_o. It was shown that the photodecarboxylation of 5*H*-dibenzo[a,d]cyclo-heptene-5-carboxylic acid (**15**) was more efficient than that of fluorene-9-carboxylic acid (**16**). Both compounds are believed to react via carbanion intermediates in S_1 (eq. 1.9 and 1.10). The intermediates **3** and **4** are the same ones formed by the deprotonation of DAD (**1**) and fluorene (**2**). Using quantum

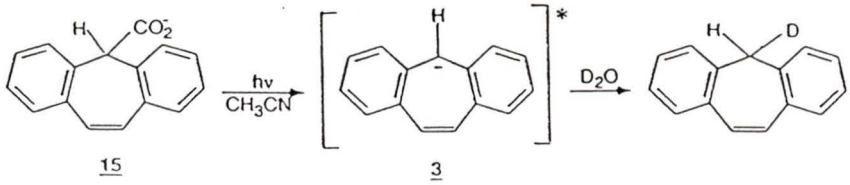

15 3

(1.9)

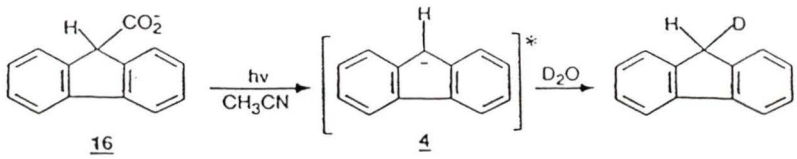

16 4

(1.10)

yields (Φ) a comparison of the photodecarboxylations involving **15** and **16** can be made. Photodecarboxylation of **15** is quite efficient with $\Phi \approx 0.6$ while **16** with $\Phi \leq 0.06$ is much less efficient. This difference is even more significant when the fluorescence lifetimes of these two species are considered. These lifetimes can be used to obtain rates for the photodecarboxylation of **15** (4.6×10^9 s^{-1}) and **16** (1.3×10^7 s^{-1}). The photoreaction involving **3** occurs at a much faster rate and is therefore more efficient. This is the result expected based on the photochemistry observed for DAD (**1**) and fluorene (**2**) (*vide supra*).

1.2.2 Rational for Behaviour of Aromatic and Antiaromatic Species in the Excited State

A simple rational for this behaviour of aromatic and antiaromatic species in the excited state can be found by comparing their electronic configurations in S_o and the

excited state. According to Hückel molecular orbital theory (HMO) the energy levels of the molecular orbitals in benzene (**12**) and cyclobutadiene (**13**) are as shown in Figure 1.9[25].

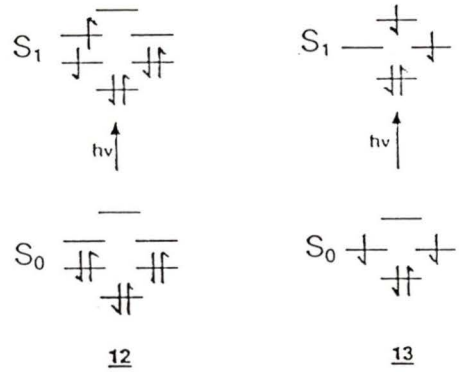

12 **13**

Figure 1.9 The molecular orbital energy levels for benzene (**12**) and cyclobutadiene (**13**) in S_o and S_1.

Benzene (**12**), with a 6π (4n+2) electronic cyclic array, is a stable species since it has a close-shell arrangement of π electrons in S_o[24]. Cyclobutadiene (**13**), has an open-shell arrangement in S_o. This is considered to be a reason for the unstable nature of cyclobutadiene (**13**) in S_o.

In S_1 a different electronic configuration exists since on excitation an electron is promoted from the highest occupied molecular orbital (HOMO) to the lowest unoccupied molecular orbital (LUMO). Benzene (**12**) loses its close-shell arrangement in S_1 and is therefore destabilized.

Cyclobutadiene (**13**) does not change after excitation as it still has an open-shell arrangement in S_1 (Fig. 1.9). This argument does not explain why delocalization of cyclobutadiene

(**13**) occurs in S_1. From this argument one would expect that **13** would exhibit the same structure and reactivity that it had in S_o or even become more localized since the orbital its electron is promoted into is antibonding.

Another argument, also based on HMO theory but which considers the true nature of cyclobutadiene, can be used to explain the behaviour of **13** in S_1. The above electronic configuration shown for **13** is for a square ring but as noted (*vide supra*) cyclobutadiene (**13**) is rectangular in S_o. Also the above electronic configuration indicates that the molecule has two unpaired electrons and a triplet ground state. Results show however that **13** has a singlet ground state and that its electrons are paired up[23]. The degeneracy of the two middle orbitals (Fig. 1.9) is therefore not entirely correct. Figure 1.10[25] is a better representation of the energy levels in **13**. The HOMO, a bonding orbital, now has two electrons and the LUMO, a similar orbital, is situated above the HOMO. Since these two orbitals are so close they are often drawn in

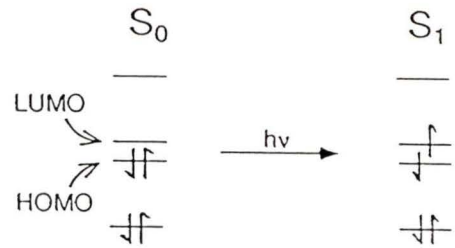

13

Figure 1.10 Corrected molecular orbital energy levels for cyclobutadiene (**13**).

as degenerate orbitals (Fig. 1.9). The LUMO of cyclobutadiene (**13**) is therefore no longer antibonding. Promotion of an electron into this new LUMO will not result in destabilization but in stabilization[2]. With both orbitals active delocalization occurs to give a square structure (Fig. 1.11)[2]. Similar arguments can be used to explain the photochemistry of DAD (**1**), fluorene (**2**) and the related carboxylic acids **15** and **16**.

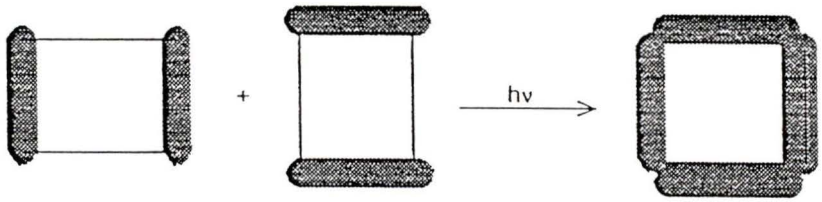

Figure 1.11 Overlap of the LUMO and HOMO of cyclobutadiene (**13**) in the excited states leading to delocalization.

DAC (**6**) is capable of forming a 8π (4n) ICA upon deprotonation like DAD (**1**). It should therefore exchange its methylene protons when photolysed in D_2O. Of course, additional photochemical processes could occur for DAC (**6**) which were not observed for DAD (**1**), such as the formal di-π-methane rearrangements described below.

1.3 Excited State Rearrangements

Two types of photochemical rearrangements are possible in

DAC (**6**). One is a true di-π-methane which produces a cyclopropyl derivative (eq. 1.11)[28]. The other, a 1,7-shift of a methylene hydrogen followed by a thermal electrocyclic ring closure, can occur to form a three membered ring as well (eq. 1.16)[29]. Emphasis will be placed on the di-π-methane rearrangement since it has been studied more extensively and is of greater relevance to photochemistry. Electrocyclic ring closures and 1,7-shifts are common to both ground and excited state chemistry. The discussion concerning the latter two will be limited to a molecule, closely related to DAC (**6**), which exhibits these rearrangements[29].

1.3.1 Di-π-methane Rearrangement

A well studied reaction in the excited state is the di-π-methane rearrangement[28]. It involves systems with π bonds separated by a saturated carbon atom, as in 1,4-pentadiene (**17**). Aryl groups, such as the one in 3-phenylpropene (**18**), may also be involved in di-π-methane rearrangements. The

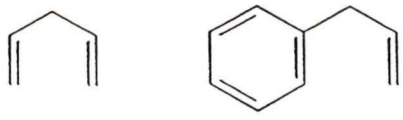

17 18

rearrangement is a radical process which can be visualized to start with the formation of a 1,4-diradical **19**. This diradical, **19**, then rearranges to give the vinylcyclopropane product **20** (eq. 1.11). Such rearrangements can occur via the

singlet or triplet state. The route taken depends on the structure of the molecule involved.

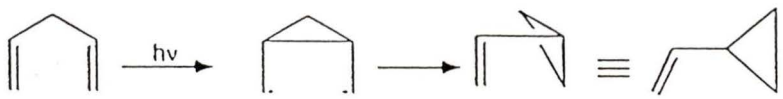

17 19 20 (1.11)

One of the first molecules shown to exhibit the di-π-methane rearrangement was barrelene (**21**). Sensitization of **21** with acetone gave semibullvalene (**22**) (eq. 1.12)[30]. Sensitization places the molecule in T_1 where it rearranges via the di-π-methane. No di-π-methane products are observed after direct irradiation of **21**, only cyclooctatetraene (**23**) (eq. 1.12). This indicates that the di-π-methane rearrangement, of barrelene (**21**), occurs in T_1 as direct irradiation would place the molecule in S_1.

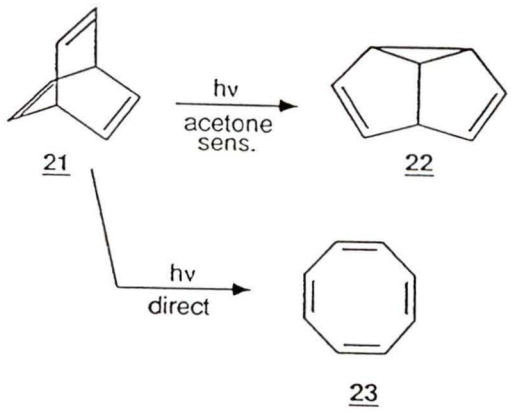

21 22 23 (1.12)

In contrast, cis-1,1-diphenyl-3,3-dimethyl-1,4-hexadiene (**24**), rearranges on direct irradiation to give the cis di-π-

methane product **25** (eq. 1.13)[31]. Direct irradiation of the trans starting material **26** produces the trans di-π-methane product **27** (eq. 1.13). However no di-π-methane products are formed after triplet sensitization of **24** only cis-trans isomerization is observed (eq. 1.13). These results indicate that acyclic systems prefer the S_1 route rather then the T_1, utilized by the bicyclic system barrelene (**21**).

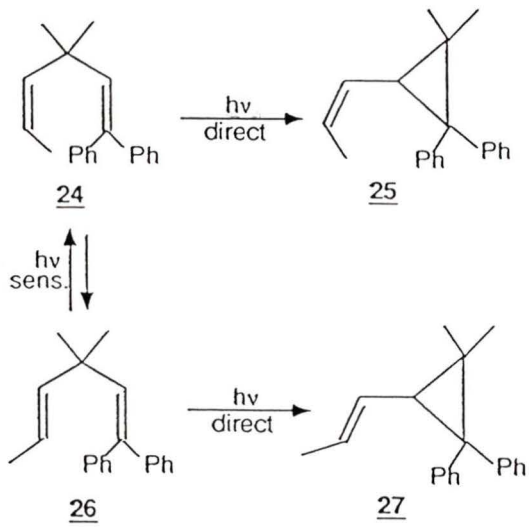

(1.13)

Numerous other examples show the same selectivity between S_1 and T_1 routes. Bicyclic molecules prefer the T_1 route while acyclic systems prefer S_1[28]. It is really not a preference for either, it is simply decided by whether there is a more efficient pathway of deactivation to the ground state. In the case of barrelene (**21**) no cis-trans isomerization can take place to deactivate molecules in T_1. In S_1 a 2+2 cycloaddition, resulting in cyclooctetraene (**23**), occurs since

this process is a more efficient deactivational pathway than the di-π-methane rearrangement. Barrelene (**21**) therefore rearranges via T_1 as no other efficient process of deactivation from T_1 exists.

In the acyclic example, the triplet route to the di-π-methane product is not observed due to the deactivation of T_1 by cis-trans isomerization. A di-π-methane rearrangement is the most efficient means of deactivation from S_1, as indicated by the absence of other processes. Acyclics in general therefore undergo the di-π-methane rearrangement in S_1.

Another important aspect of di-π-methane rearrangements is that they are highly regiospecific regarding which π group will remain unchanged and which will change to produce a three membered ring[28]. This selectivity results from the stabilization of the radical intermediates involved. In the third example, involving cis-1,1-diphenyl-3,3-dimethyl-1,4-hexadiene (**24**), it was seen that the π group situated in the dibenzylic position disappears to form the vinylcyclopropane[30]. This is due to the benzylic radical being stabilized by delocalization. The other radical, being less stable, will promote the homolytic cleavage of the adjacent bond in the 1,4-diradical **28**, leading to a 1,3-diradical **29**. This can close up to give the vinylcyclopropane product **25** (eq. 1.14).

A reverse effect is seen for di-π-methane rearrangements involving aromatic π groups[28]. Rearomatization is the factor which controls the regiospecificity of these systems, as

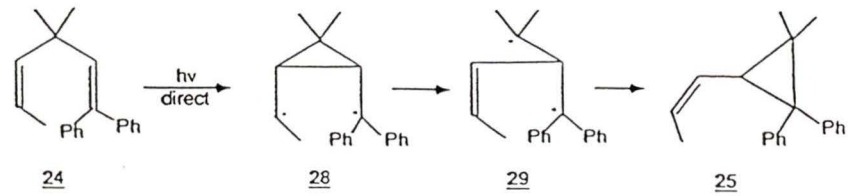

24 28 29 25 (1.14)

demonstrated by 3,3,3-triphenylpropene (**30**)[32]. Rearrangement of the initial diradical species **31**, is promoted by rearomatization. The diradical left **32**, closes up giving triphenyl cyclopropane **33** (eq. 1.15).

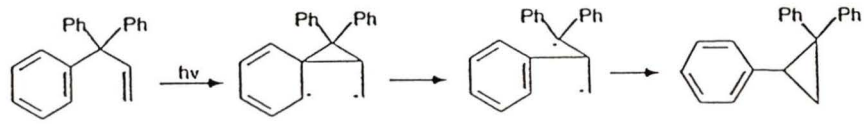

30 31 32 33 (1.15)

Bicyclic systems also exhibit the regiospecificity demonstrated by the above acyclic examples[28].

1.3.2 1,2-Benzotropilidene (34)

The other rearrangement expected for DAC (**6**) can be demonstrated by using a related system, 1,2-benzotropilidene (**34**). Direct photolysis of **34** (eq. 1.16) gives benzonorcaradiene (**36**), via a 1,7-hydrogen shift followed by an electrocyclic ring closure[29,33]. The 1,7-hydrogen shift gives the intermediate **35**, which then undergoes a thermal disrotatory electrocyclic ring closure producing the final product **36**. Evidence supporting this mechanism was

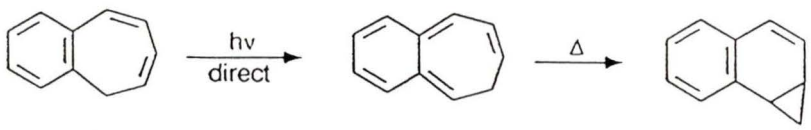

34 35 36 **(1.16)**

provided by the direct photolysis of the tetra-deuterated species **37** (Scheme 1.3). The location of the deuterium in product **38**, indicates that product **36** was not formed by a di-π-methane rearrangement. This type of rearrangement would place the deuterium as shown in **39**. Therefore deactivation of 1,2-benzotropilidene (**34**) from S_1 occurs via a more efficient 1,7-hydrogen shift rather then a di-π-methane rearrangement.

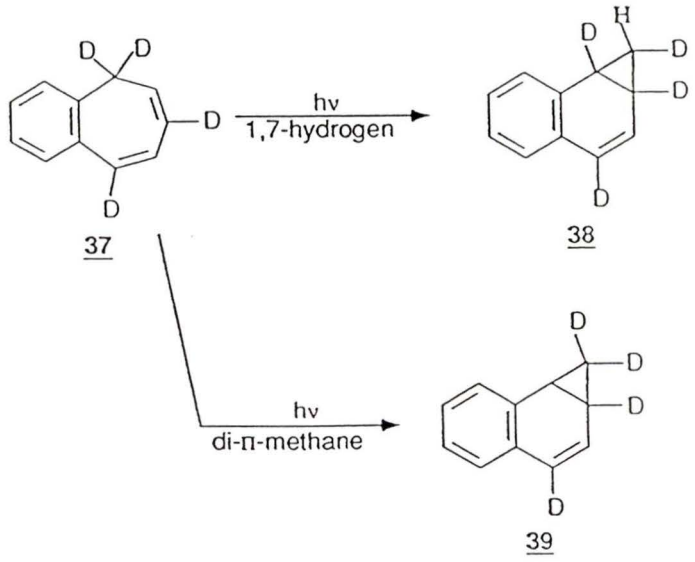

Scheme 1.3

Triplet sensitization of 1,2-benzotropilidene (**34**) does not lead to the same product as above but results only in isomerization of the molecule to 3,4-benzotropilidene (**40**)

(eq. 1.17)[29,33]. As before the di-π-methane rearrangement is disallowed by another more efficient pathway of deactivation. If this isomerization process was restricted a di-π-methane rearrangement could occur via the triplet state.

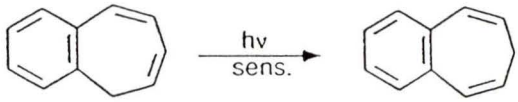

34 40 **(1.17)**

1.4 Proposed Research

DAC (**6**), like DAD (**1**), is capable of forming an 8π ICA upon deprotonation. However, the placement of its aromatic rings may lead to other photochemical processes not observed in DAD (**1**). The purpose of this research is to determine the extent of each photochemical process, how they affect each other and the mechanisms by which they occur.

Photolysis of DAC (**6**) in various solvents will first be carried out to determine its photochemical behaviour. Any photochemical processes observed could occur via S_1 or T_1. Triplet sensitization of DAC (**6**) will therefore be carried out to determine which excited state each process arises from. Quantum yields will then be measured to quantify each process.

Any formal di-π-methane product observed in the above photolysis could occur via a di-π-methane rearrangement and/or a 1,7-hydrogen shift. The mechanism involved will be

determined by the photolysis of deuterium labelled DAC (**6**). The location of the deuterium in the products should indicate the mechanism involved.

The mechanism of the photochemical proton exchange will in turn be investigated utilizing steady state fluorescence studies. These studies should also provide an estimate for the change in pK_a of DAC (**6**) after excitation.

CHAPTER 2

RESULTS AND DISCUSSION

2.1 Synthesis

2.1.1 5*H*-Dibenzo[a,c]cycloheptene (6)

DAC (**6**) was synthesized according to the method outlined in Scheme 2.1. Ketone **42** was prepared from diphenic anhydride **41** in several steps, according to the procedure of Tolbert and Ali[34] . Reduction of the ketone **42** to the alcohol **43** was then accomplished using $NaBH_4$. Refluxing **43** in H_3PO_4 furnished the dehydration product, DAC (**6**). Purification was accomplished by bulb-to-bulb distillation, which provided an oil consisting of >99% DAC (**6**) by gas chromatography (GC).

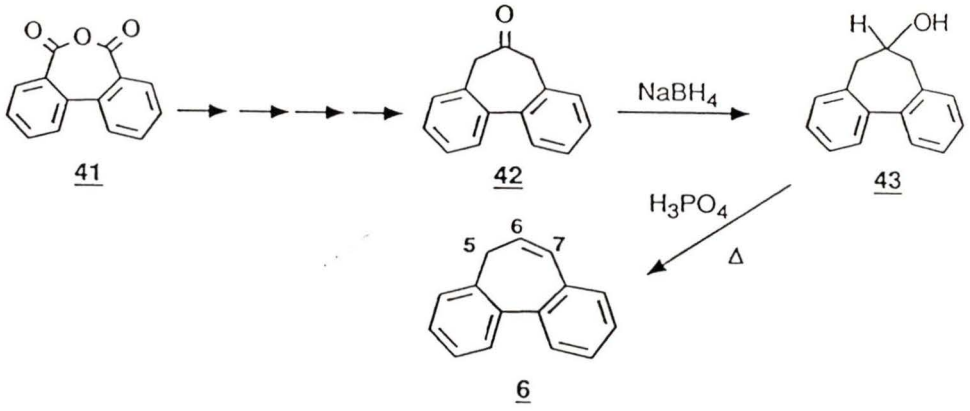

Scheme 2.1

The ^1H NMR (90 MHz and 360 MHz) spectrum of the purified DAC (**6**) agreed with the literature spectrum[35]. The ^{13}C NMR also indicated the required product. The literature UV spectrum[36] was found to differ somewhat from the spectrum obtained for the above material. The absorption maxima were in agreement but the extinction coefficients were dissimilar

(Table 2.1). Further confirmation of the product's identity was obtained by analysis of its mass spectrum (MS). The expected molecular weight of DAC (**6**) (192 atomic mass units) was observed.

Table 2.1 Experimental and Literature[36] UV data for DAC (**6**).

Literature (EtOH)		Experimental (CH_3CN)	
λ_{max} (nm)	ϵ (L mol^{-1} cm^{-1})	λ_{max} (nm)	ϵ** (L mol^{-1} cm^{-1})
243.5	7300	233	38400
251.5*	2670	250*	13700
296*	256	290*	1300

*Shoulder

**Average of 3 runs except value for 290 nm shoulder (estimated error ± 10%).

2.1.2 6-Deuterio-5*H*-dibenzo[a,c]cycloheptene (46)

Deuterium labelled DAC (**6**) was required for studies of the formal di-π-methane rearrangement. Ketone **42** was reduced with $NaBD_4$ to place a deuterium at the position shown in alcohol **44** (Scheme 2.2). Dehydration utilizing H_3PO_4 was not viable as it led to exchange of the deuterium. Bromination of alcohol **43** with PBr_3 gave **45** which on treatment with 3 M KOH gave two major products. One was the required 6-deuterio-5*H*-dibenzo[a,c]cycloheptene (6DDAC) (**46**) (64%), the other was 9-

methylphenanthrene (**47**) (36%).

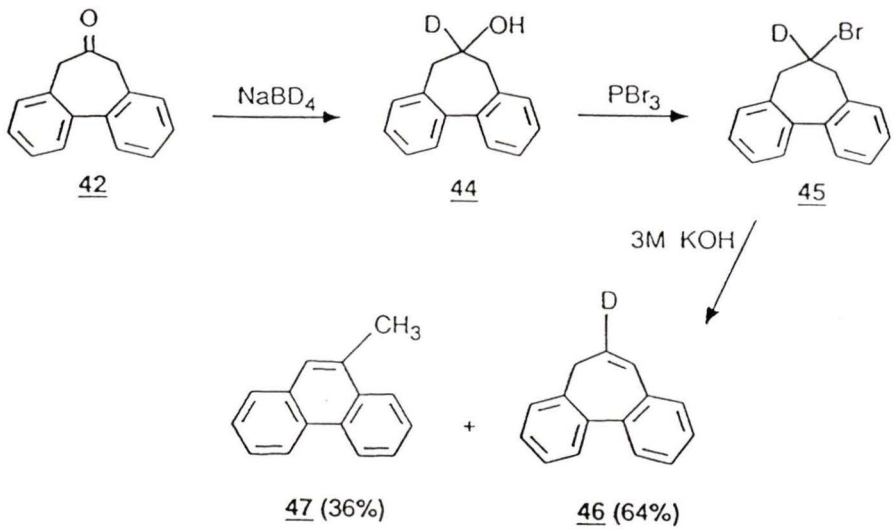

Scheme 2.2

Separation of **46** from **47** by bulb-to-bulb distillation was unsuccessful. Preparative High Performance Liquid Chromatography (HPLC) was used to isolate 6DDAC (**46**) with a purity of 90%, as indicated by GC/MS. The same GC/MS also indicated the presence of DAC (**6**) (≈4%) and 9-methyl-phenanthrene (**47**) (≈6%) as contaminants.

The ^{1}H NMR (360 MHz) of 6DDAC (**46**) confirmed that the deuterium was located at position 6. With a deuterium in this position the protons in positions 5 and 7 are not split into doublets but appear as singlets. A small peak at 6.2-6.3 ppm indicated the presence of the impurity DAC (**6**). The presence of the other impurity, **47**, was confirmed by the methyl signal at 2.76 ppm[37]. However, examination of the regions in the ^{1}H NMR of 6DDAC (**46**) where products from the formal di-π-methane rearrangement were expected showed no interfering peaks.

Therefore the impurities would not interfere with the mechanistic studies. This material was therefore used for the rearrangement studies (*vide infra*).

2.2 Photolysis of DAC (6)

2.2.1 Direct Irradiation of DAC (6) in D_2O

Direct irradiation of an argon purged solution of DAC (**6**) ($5x10^{-4}$ moles) in 100 mL 50% D_2O-CH_3CN with a Rayonet RPR 100 photochemical reactor (254nm lamps) at ≈17°C for 30 minutes gave the products shown in eq. 2.1, according to GC/MS.

The ^1H NMR (90 MHz) of the product mixture indicated the presence of 5-deuterio-5*H*-dibenzo[a,c]cycloheptene (5DDAC) (**48**) and the formal di-π-methane product, dibenzonorcaradiene

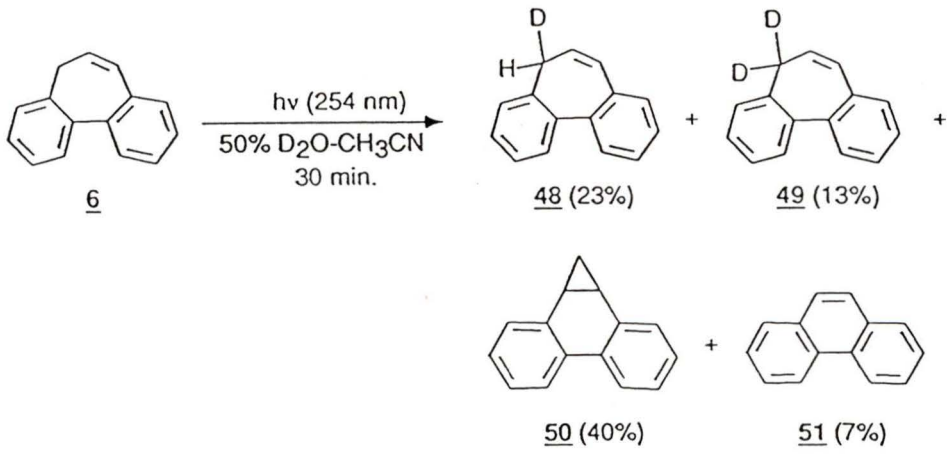

(2.1)

(DBN) (**50**). Deuterium incorporation at position 5 was indicated by the reduction in size of the methylene peak at 3.0 ppm. Formation of either or both of **48** and 5,5-dideuteriodibenzo[a,c]cycloheptene (5DDDAC) (**49**) could account

for this reduction.

If the carbanion, formed upon deprotonation, is delocalized, then one would expect that positions 5 and 7 would become equivalent. Incorporation of a deuterium should occur at either position to give 5DDAC (**48**). A second deprotonation would then result in deuterium incorporation at position 5 or 7 as in **49** and **52** (eq. 2.2). Products **52** and **49** are difficult to identify in the ^{1}H NMR since the regions in which their protons resonate are obscured by other resonances.

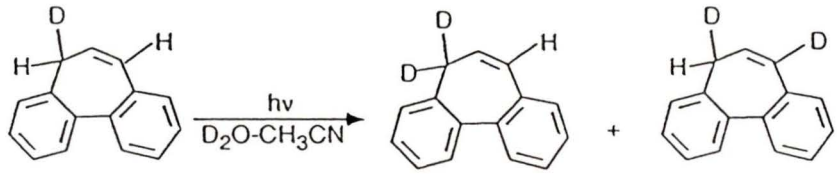

48 49 52 (2.2)

Exchange at position 7 could be confirmed by the photolysis of 7-deuterio-5*H*-dibenzo[a,c]cycloheptene (**53**) in H_2O (eq. 2.3). If position seven was involved in the proton exchange, the deuterium in position seven would be exchanged off.

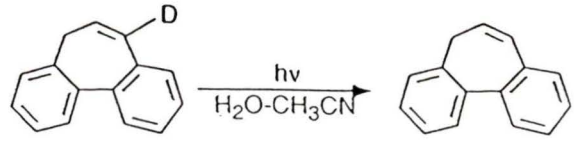

53 6 (2.3)

The GC/MS indicated that deuterium was incorporated into DBN (**50**). Subsequent photolysis of 5DDAC (**48**) must have occurred to give the rearranged product containing deuterium. The yields for exchange are then higher than the above results

indicate.

The presence of DBN (**50**) in the photoproducts was verified by comparing its spectrum with the literature ^{1}H NMR spectrum[38]. The other product, phenanthrene (**51**), is a secondary photoproduct resulting from photolysis of DBN (**50**). This was demonstrated by Richardson et. al.[39] who photolysed DBN (**50**) and obtained **51** as the major product.

2.2.2 Direct Irradiation of DAC (6) in CH_3CN

Photolysis of DAC (**6**) in pure CH_3CN, following the above procedure, resulted in DBN (**50**) and phenanthrene (**51**) (eq. 2.4). The photoproducts obtained were analyzed by ^{1}H NMR (360 MHz) which indicated the yields shown. When a comparison of

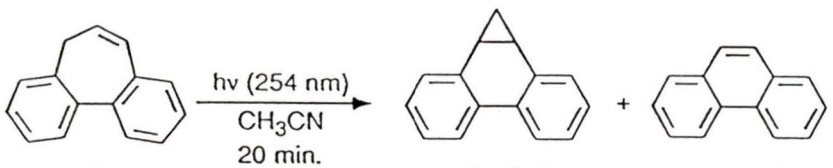

6 50 (67%) 51 (15%) (2.4)

the yield for DBN (**50**) in D_2O–CH_3CN versus CH_3CN is done one can see that in the absence of water the rearrangement process is more efficient. The exchange process therefore must compete with the rearrangement process for deactivation of excited DAC (**6**). These results however do not rule out the possibility of exchange in CH_3CN since deuterated species were not involved in the last photolysis.

To confirm that exchange did not occur in pure CH_3CN, DAC

(**6**) was irradiation in CD_3CN. A small scale photolysis was preformed in this case as CD_3CN is quite expensive. On an optical bench a 3 mL solution of DAC (**6**) (6.43×10^{-7} moles) in CD_3CN was purged with argon and then photolysed for 60 minutes with a mercury arc lamp (280 nm). A long photolysis is required on the optical bench since the intensity of the light source is much less then that in the photochemical reactor. The resulting mixture was analyzed by GC/MS and indicated that no exchange took place in CD_3CN (eq. 2.5). This result is

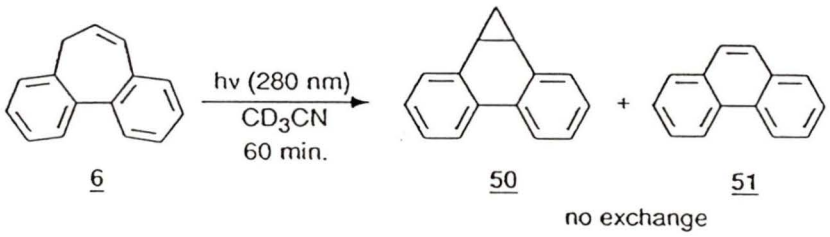

(2.5)

important as it indicates that the exchange is not occurring by a radical process (Scheme 2.3). If this were the case the

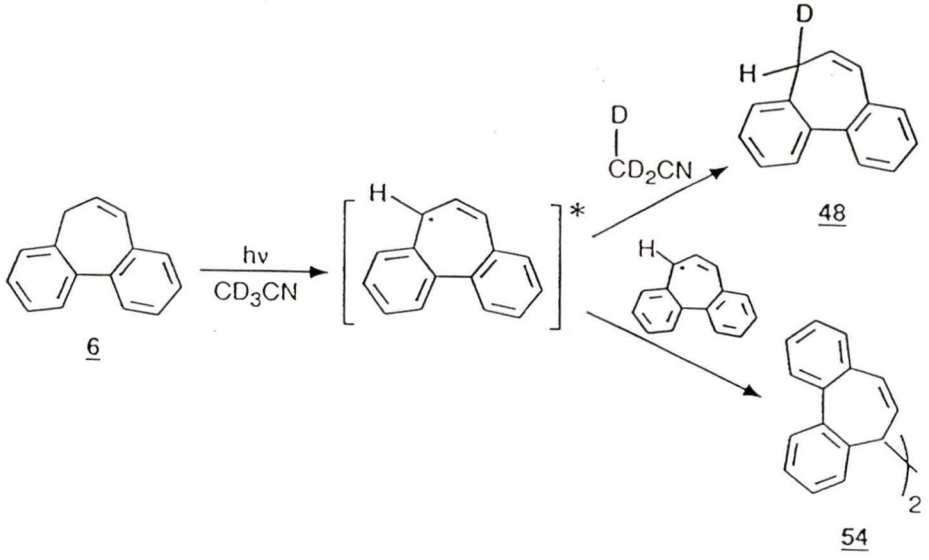

Scheme 2.3

radical intermediate formed after excitation would have picked up a deuterium from CD_3CN since its C-D bond strength (86 kcal $mole^{-1}$)[40] is weaker than the O-D bond (119 kcal $mole^{-1}$)[40] of D_2O. Radical processes also lead to dimerization however no bis-5*H*-dibenzo[a,c]cycloheptene (**54**) was observed in the proton NMR or GC/MS. The exchange process of DAC (**6**) is therefore believed to go via carbanion **55**, with an 8π ICA similar to the one proposed for DAD (**1**).

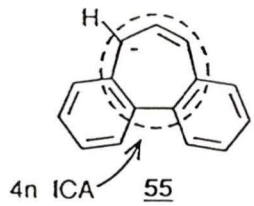

To confirm that the processes observed for DAC (**6**) only occurred in the excited state a dark control reaction was preformed. The conditions utilized for the photolysis of DAC (**6**) in CD_3CN were repeated except 50% D_2O-CH_3CN was used and no irradiation was done. Only DAC (**6**) was observed by GC/MS after several hours in the dark.

2.2.3 Triplet Sensitization of DAC (6)

The proton exchange observed for DAC (**6**) and the formal di-π-methane rearrangement could originate from either S_1 or T_1. To determine the extent of S_1 and T_1 reactivity, triplet sensitization of DAC (**6**) was carried out.

Triplet sensitization is a photochemical process used to

selectively place a molecule in its T_1 state by energy transfer[9]. In order for energy transfer (ET) to occur, the sensitizer (donor) utilized must have a T_1 state with an energy higher than the T_1 energy of the molecule to be sensitized (acceptor) (Fig. 2.1). Benzoylbenzoic acid (**56**) was chosen as the triplet sensitizer for DAC (**6**) since benzophenones have a triplet energy (E_T) of 68-71 kcal mol^{-1} [40]. An E_T for DAC (**6**) of ≈60 kcal mol^{-1} was estimated by using styrene which has a similar chromophore and an E_T of 62 kcal $mole^{-1}$ [40].

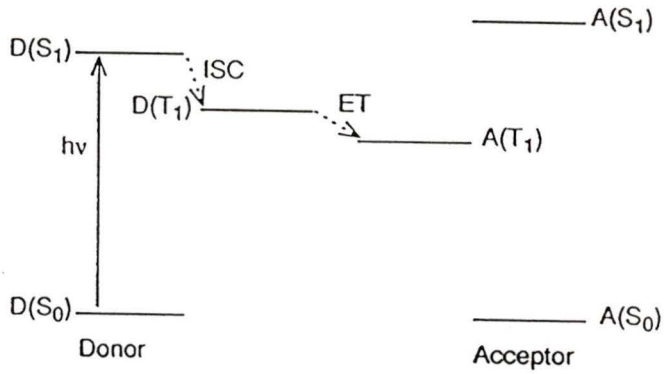

Figure 2.1 Relative energies of the triplet states of the donor and acceptor required for triplet sensitization, where ISC indicates intersystem crossing (*vide infra*)

Using a Rayonet RPR 100 photochemical reactor (350nm lamps) a 100 mL CH_3CN solution containing DAC (**6**) ($5x10^{-5}$moles) and benzoylbenzoic acid (**56**) ($3x10^{-3}$moles) was photolysed for 10 minutes in a pyrex tube well purging with argon (eq 2.6). A pyrex tube, 350 nm lamps and a large excess of **56** were used

to insure that only the sensitizer was being excited. Under such conditions direct excitation of DAC (**6**) was impossible as it absorbs below 310 nm.

The product isolated (eq. 2.6) can then only originate from T_1. One product, DBN (**50**), was observed in the proton NMR (90 MHz) and GC of the photoproducts. The formal di-π-methane rearrangement resulting in DBN (**50**) can therefore originate from T_1. This does not indicate that a similar rearrangement could not occur via S_1, as the rearrangement could occur in both excited states.

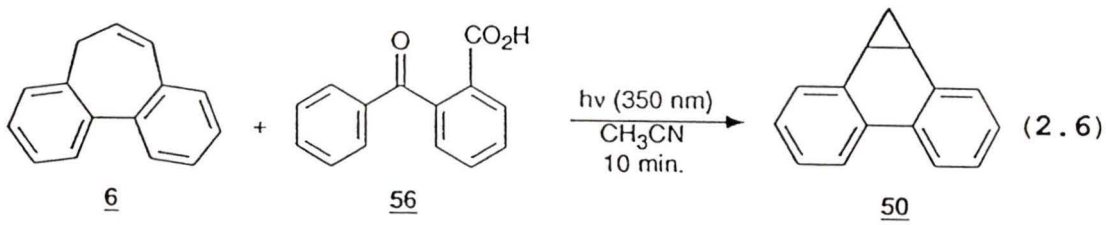

6 + 56 → 50 (2.6)

In order to determine which state the proton exchange observed for DAC (**6**) originated from, the above triplet sensitization was repeated in 50% D_2O-CH_3CN for 30 minutes. Analysis of the resulting mixture by GC/MS indicated that no exchange took place only rearrangement (eq. 2.7).

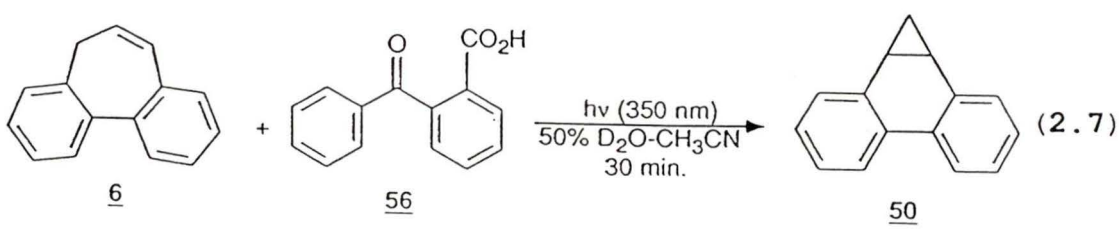

6 + 56 → 50 (2.7)

The proton exchange observed for DAC (**6**) therefore occurs

via S_1. This result was expected since, differences in pK_a between S_1 and S_0 are in general larger than the differences in pK_a between T_1 and S_0[13]. A large change in pK_a is believed to occur since the methylene protons of DAC (**6**) are exchanged in the excited state but have a pK_a of ≈32-36[5] in the ground state.

2.2.4 Product Quantum Yields

Photochemical reactions are quantified by the measurement of product quantum yields (Φ_p), which are a measure of the number of moles of photoproducts produced per mole (or Einstein) of radiation absorbed[9].

$$\frac{\text{moles of photoproduct}}{\text{Einsteins of light absorbed}} = \Phi_P$$

Several product quantum yield values were required to quantify the photochemical reactions of DAC (**6**). Measurement of the quantum yields for proton exchange and formal di-π-methane rearrangement were performed. The quantum yields were obtained on an optical bench utilizing a mercury arc lamp in conjunction with a monochromator to obtain an excitation wavelength of 280 nm. Samples were irradiated in UV cuvettes while purging with argon. The Einsteins emitted by the light source per a minute were measured with a Potassium Ferrioxalate ($K_3[Fe(C_2O_4)_3]\cdot 3H_2O$) Chemical Actinometer[40,41].

Table 2.2 lists the quantum yields measured for the proton exchange and the formal di-π-methane rearrangement of

DAC (**6**) in various solvents. These results indicate that the photochemistry of DAC (**6**) is solvent dependent.

Table 2.2 Quantum yields for proton exchange (Φ_{ex}) and cyclization (Φ_{cycl}) of DAC (**6**) in various solvents.

Solvent	Φ_{cycl}	Φ_{ex}
CH_3CN	0.087±0.004	--
C_6H_{12}	0.015±0.001	--
70% H_2O-CH_3CN	0.009±0.001	--
70% CH_3OD-CH_3CN	0.007±0.001	0.007±0.001
70% D_2O-CH_3CN	0.012±0.001	0.034±0.006

Only the formal di-π-methane rearrangement is observed in the aprotic solvents CH_3CN and cyclohexane (C_6H_{12}). In the presence of a protic solvent (D_2O) the proton exchange dominates the photochemistry observed for DAC (**6**).

In C_6H_{12} rearrangement occurs but to a small extent compared to that seen in CH_3CN. This may indicate that the rearrangement process is solvent dependent since C_6H_{12} is a less polar solvent then CH_3CN[21].

With CH_3OD–CH_3CN both proton exchange and rearrangement occur inefficiently. The solvent CH_3OD was used to determine if other protic solvents could affect the proton exchange of DAC (**6**). The low quantum yield for exchange was expected since CH_3OD has a much lower dielectric constant then D_2O[42].

CH_3OD is also bulkier and has only one deuterium available for exchange. The low result for the formal di-π-methane rearrangement however was unexpected since with a reduction in the rate of proton exchange one would expect the rate of the competing rearrangement to increase. Once again the low quantum yield for the rearrangement in CH_3OD may indicate that the formal di-π-methane rearrangement is solvent dependent.

Before all these results can be interpreted, further studies of DAC (**6**) are required. Discussion of the solvent affects will therefore be delayed to the end of the next section which deals with the mechanism of the formal di-π-methane rearrangement.

2.3 Mechanism of the Formal Di-π-methane Rearrangement

Photolysis of 6DDAC (**46**) with subsequent ^1H NMR analysis should reveal the mechanism of the formal di-π-methane rearrangement. Both the true di-π-methane rearrangement and the 1,7-hydrogen shift with electrocyclic ring closure are possible. The two rearrangements can, however, be differentiated since the position of the deuterium in the photoproducts of 6DDAC (**46**), depends on the mechanism involved (Scheme 2.4).

The di-π-methane rearrangement results in the deuterium being located at the methine position of the cyclopropyl ring (protons H_A). Such a rearrangement would be expected to occur via T_1 since deactivation of this state by isomerization as in

34 is not possible in DAC (**6**).

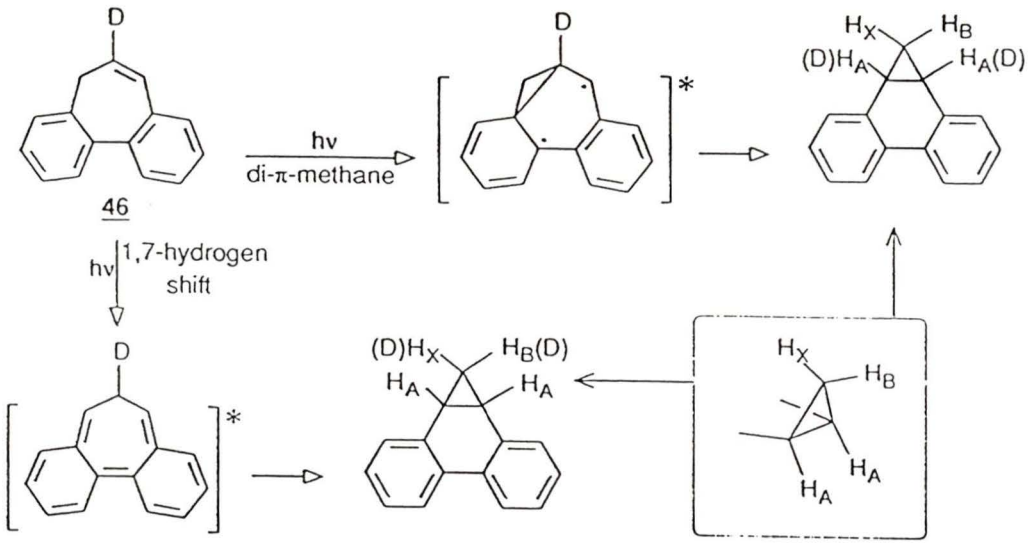

Scheme 2.4

If the 1,7-hydrogen shift occurs, the deuterium would be located at the methylene position of the cyclopropyl ring in DBN (**50**). Two types of protons exist at the methylene position (H_X and H_B) since this position is bent out of the plane of the six membered ring[39]. The disrotatory electrocyclic ring closure can place the methylene carbon up or down (Scheme 2.4)[29]. Therefore the deuterium can be located in either position H_X or H_B. If the 1,7-hydrogen shift is observed in DAC (**6**) it would be expected to occur via S_1 since this is the excited state in which the rearrangement of **34** occurs[29].

2.3.1 Direct Photolysis of 6DDAC (48) in CH_3CN

Direct irradiation of an argon purged CH_3CN solution of 6DDAC (**46**) ($\approx 2 \times 10^{-4}$ moles) at ≈17°C in a photochemical reactor

(254 nm lamps) for 20 minutes provided several products (eq. 2.8). A rough estimate for the relative yield of each product was obtained by comparing the intensities of the peaks observed for each product in the ^{1}H NMR (360 MHz) (Fig 2.3).

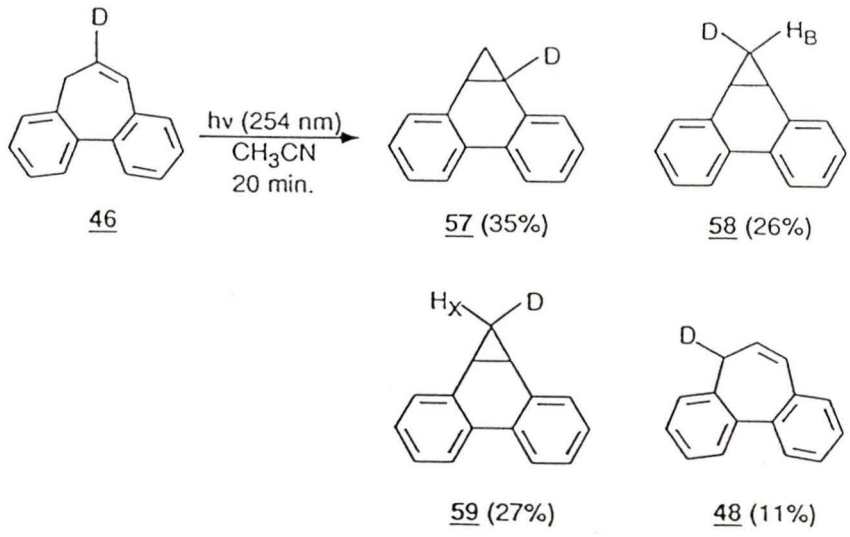

46 57 (35%) 58 (26%) 59 (27%) 48 (11%) **(2.8)**

Both the di-π-methane and 1,7-hydrogen shift products were obtained, indicating that both mechanisms operated in CH_3CN. This was determined by looking for the splitting patterns and coupling constants (J in Hz) expected for H_A, H_B and H_X in each of the products. The coupling constants expected between the protons (Table 2.3) were determined from the ^{1}H NMR (360 MHz) of DBN (**50**) (Fig. 2.2). With these coupling constants the splitting pattern for each proton of the products were predicted. Deuterium coupling is generally less then 1 Hz and only results in the broadening of signals[43], it therefore has little effect on the splitting patterns. The ^{1}H NMR observed was then compared to the predicted spectrum to

identify each product.

Table 2.3 Data from the ^1H NMR of DBN (**50**).

DBN (50)	δ (ppm)	multiplicity	J (Hz)
H_A	2.57	dd	8.9,4.9
H_B	1.58	td	8.9,3.9
H_X	-0.05	td	4.9,3.9

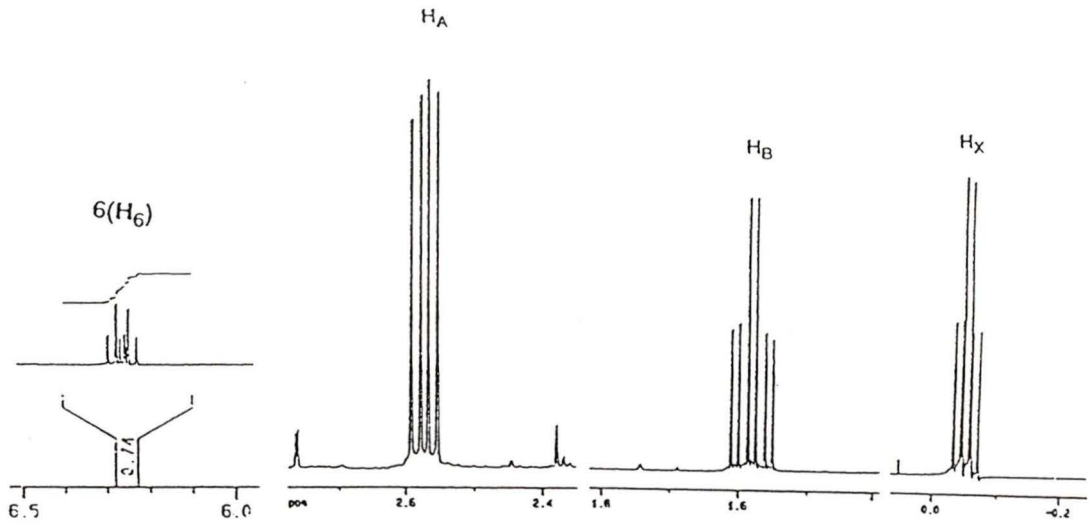

Figure 2.2 ^1H NMR of H_A, H_B and H_X in DBN (**50**) obtained from the direct photolysis of DAC (**6**) in CH_3CN. H_6 of DAC (**6**) is also shown for a comparison to be made later.

Product **57** from the di-π-methane rearrangement was difficult to identify since all the splitting patterns due to coupling of its protons H_A, H_B and H_X are doublets of doublets. No large peaks therefore stand out in the multiplets to indicate the presence of **57** (Fig. 2.3). Peaks identified as

being due to **57** had coupling constants which compared well with the expected values (Table 2.4).

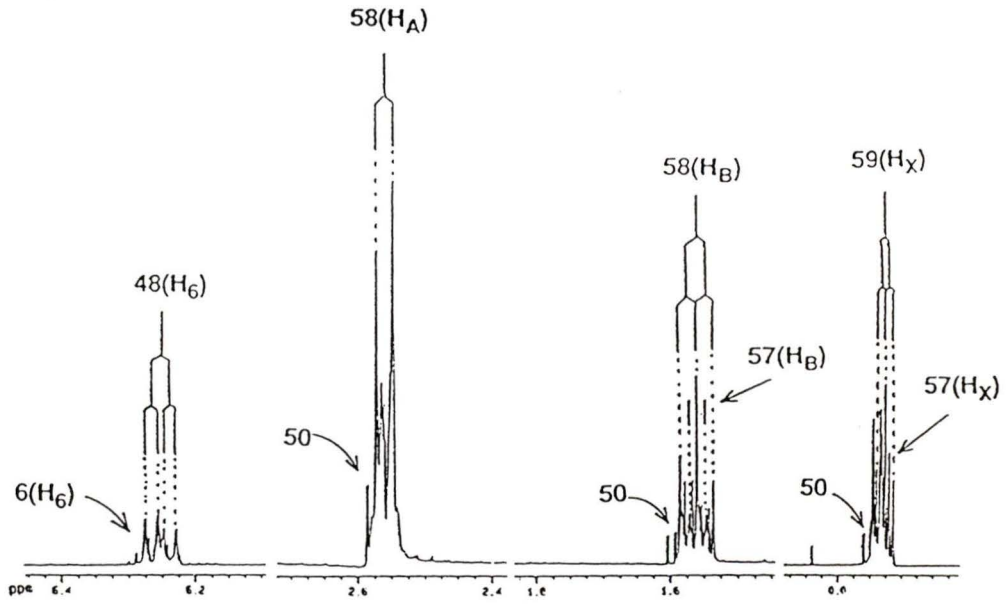

Figure 2.3 Regions of the ^{1}H NMR (from the direct photolysis of 6DDAC (**46**) in CH_3CN) where H_A, H_B, H_X and H_6 resonate.

The two products from the 1,7-hydrogen shift were simpler to find since the splitting patterns for these products produce several strong peaks (Fig. 2.3). Product **58** (H_X=D) is expected to give a doublet for H_A at ≈2.56 ppm and one is observed in the region 2.53-2.59 ppm with the correct coupling constant. Product **59** (H_B=D) should also give a doublet in this region but it is partially hidden by the doublet from **58**. The doublet of **59** is weaker then the doublet due to **58** because as will be seen in subsequent spectra the deuterium at H_B

broadens the H_A resonance more than would a deuterium in the position H_X. The other regions of the spectrum confirmed the presence of **58** and **59**. A triplet was predicted for H_B of **58** and one is clearly visible at 1.56 ppm with the correct coupling constant. A triplet is also expected for H_X of **59** and one is observed at ≈−0.07 ppm, again with the correct coupling constant (Table 2.4).

Table 2.4 Observed splitting patterns and coupling constants from Figure 2.3 for products **57, 58** and **59**.

Comp #	H	multiplicity	J (Hz)
57	H_A	dd	?
	H_B	dd	8.9,3.9
	H_X	dd	?,3.9
58	H_A	d	8.8
	H_B	t	8.9
	H_X	-	-
59	H_A	d	?
	H_B	-	-
	H_X	t	4.9

Other peaks appear in the regions where H_A, H_B and H_X resonate. They are due to nondeuterated DBN (**50**) which results from the photolysis of the impurity DAC (**6**).

The fourth product **48** resulting from the photolysis of 6DDAC (**46**) was discovered in the region where the proton in

position 6 of DAC (**6**) resonates (6.2-6.3 ppm). In this region one would expect a doublet of triplets due to the impurity DAC (**6**) (Fig. 2.2). This splitting pattern is seen but overlapping it is a doublet of doublets expected for H_6 of **48** (Fig. 2.3). Reversal of the 1,7-hydrogen shift would give **48** if the deuterium of position 6 was moved to position 5 (Scheme 2.5). Such a reversal is possible as it is observed in a related system cycloheptatriene (**60**) (*vide infra*)[44]. Subsequent photolysis of **48** would give the product expected for a di-π-methane rearrangement but via the 1,7-hydrogen shift. The di-π-methane product obtained above could therefore have resulted from this series of photolysis.

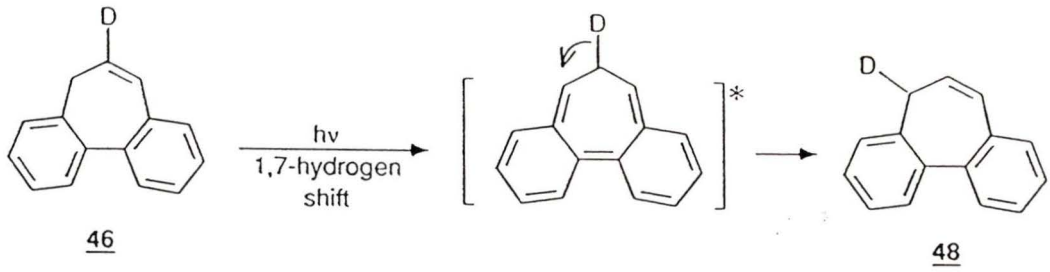

46 48

Scheme 2.5

To eliminate this possibility a shorter photolysis was done. Analysis of the photoproducts by ^1H NMR (360 MHz) gave the same ratios of products observed in the above photolysis. It is highly unlikely that a substantial amount of material could undergo a two photon reaction during a short photolysis. Therefore both the di-π-methane rearrangement and the 1,7-hydrogen shift occur on direct irradiation of 6DDAC (**46**) in CH_3CN.

2.3.2 Triplet Sensitization of 6DDAC (46)

Following the same procedure outlined for the triplet sensitization of DAC (**6**) (*vide supra*), 6DDAC (**46**) ($\approx 2 \times 10^{-4}$ moles) was sensitized to determine which formal di-π-methane mechanism operated via T_1. Analysis of the product mixture by ^1H NMR (360 MHz) (Fig. 2.4) indicated one product (eq. 2.9).

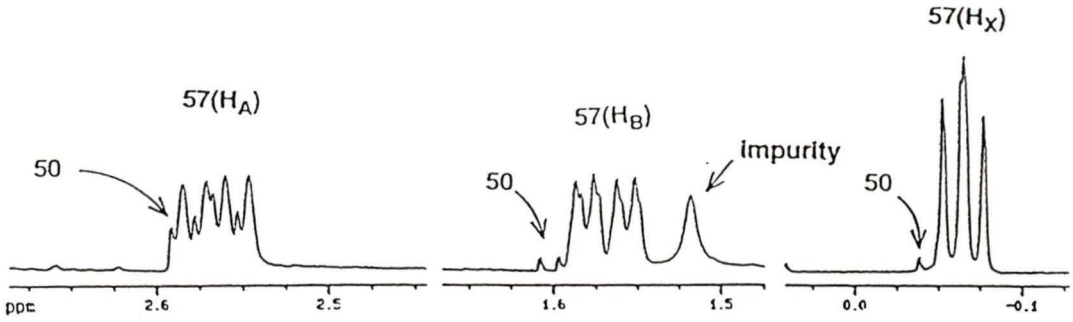

Figure 2.4 Regions of the ^1H NMR (from the triplet sensitization of 6DDAC (**46**)) where H_A, H_B and H_X resonate.

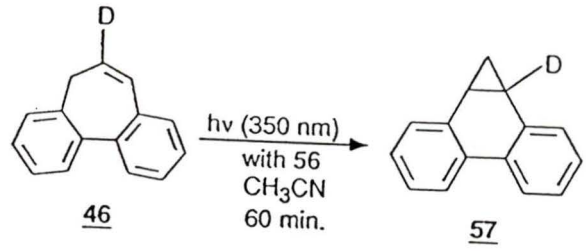

(2.9)

The location of the deuterium was again determined from the splitting patterns and coupling constants observed in the regions where H_A, H_B and H_X resonate. As indicated above all the cyclopropyl protons of **57** are split into doublets of doublets. Both H_A and H_B exhibit this splitting pattern but H_X resembles a distorted triplet (Fig. 2.4). This is expected since the two center peaks for the doublet of doublet produced

by H_X overlap giving three peaks instead of four. The coupling constants observed in each splitting pattern agree with the expected values (Table 2.5).

Table 2.5 Observed splitting patterns and coupling constants from Figure 2.4 for product **57**.

Comp #	H	multiplicity	J (Hz)
57	H_A	dd	8.9,4.9
	H_B	dd	8.9,3.9
	H_X	dd	?

By looking at the relative intensity of the peaks for each proton of the three membered ring one would expect a 1:1:1 ratio since each arises from one proton. However, the H_X resonance is sharper and more intense than the resonances for H_A and H_B (Fig. 2.4). The reason for this was pointed out earlier in the comparison of the doublets observed for the 1,7-hydrogen shift products **58** and **59** (Fig. 2.3). The same situation exists in this molecule since the deuterium is located on the same face of the three membered ring as H_A and H_B. H_A and H_B are therefore broadened by the deuterium since coupling is stronger between protons on the same face of the three membered ring. H_X is not located on the same face as the deuterium and therefore it gives rise to sharper peaks.

Product **57** from the triplet sensitization of 6DDAC (**46**) indicates that the di-π-methane rearrangement operates in T_1.

However, this result does not indicate that the di-π-methane rearrangement only occurs in the triplet state. It could still occur with the 1,7-hydrogen shift in the singlet state.

2.3.3 Triplet Quenching of 6DDAC (46)

To determine which formal di-π-methane rearrangement was occurring via the singlet state, 6DDAC (**46**) was photolysed in the presence of a triplet quencher[14] (eq. 2.10). The procedure utilized in the direct photolysis of 6DDAC (**46**) was repeated, except the system was purged with oxygen. Oxygen acts as a triplet quencher preventing rearrangements via T_1[14]. Results from the analysis of the product mixture by ^{1}H NMR (360 MHz) were questionable as the quantity of product isolated was quite small. As well, several impurities existed which overlapped the regions of interest (Fig. 2.5).

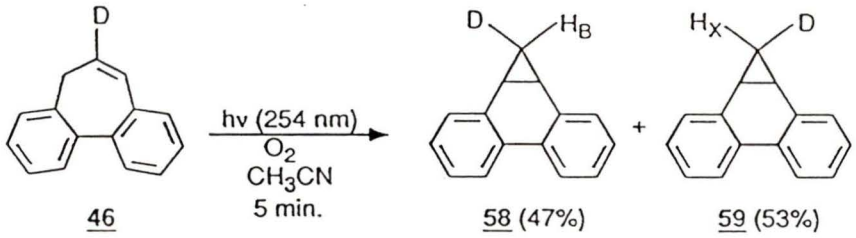

46 58 (47%) 59 (53%) **(2.10)**

The products expected via the 1,7-hydrogen shift (**58** and **59**) were both visible in the ^{1}H NMR (Fig. 2.5). The overlapping doublets expected for H_A coupling to H_B in **58** and H_X in **59** are visible at 2.5-2.6 ppm. In the regions where H_B and H_X resonate impurities existed making the interpretation of the ^{1}H NMR difficult. Portions of the triplets expected in

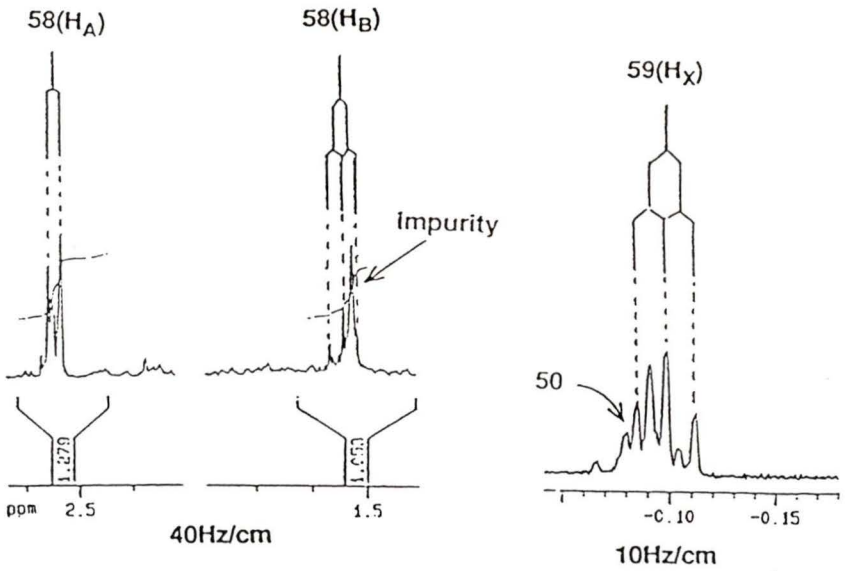

Figure 2.5 Regions of the ^1H NMR (from the triplet quenching of 6DDAC (**46**)) where H_A, H_B and H_X resonate.

these regions are visible. The coupling constants obtained from these triplets agree with the expected values (Table 2.6). One can not say that these are the only products, as

Table 2.6 Observed splitting patterns and coupling constants from Figure 2.5 for products **58** and **59**.

Comp #	H	multiplicity	J (Hz)
58	H_A	d	8.8
	H_B	t	8.9
	H_X	-	-
59	H_A	d	?
	H_B	-	-
	H_X	t	4.9

the spectrum is weak and the regions of interest are obscured by other resonances. Further triplet quenching studies are required to determine whether or not both formal di-π-methane rearrangements operate in S_1.

The quantum yields measured earlier (Table 2.2) demonstrated that these formal di-π-methane rearrangements were effected by the nature of the solvent. Di-π-methane rearrangements are not considered solvent dependent and are generally preformed in non-polar solvents such as C_6H_{12}[28]. Electrocyclic ring closures and 1,7-hydrogen shifts are also not solvent dependent, to a large extent, since both are concerted processes[45]. In 1,2-benzotropilidene (**34**) and 3,4-benzotroplidene (**40**) (*vide supra*) the 1,7-hydrogen shift is not effected by the solvent since the quantum yields for rearrangement in C_6H_{12}, CH_3CN, and H_2O-CH_3CN are all ≥ 0.7[46]. However the quantum yield for rearrangement of DAC (**6**) in C_6H_{12} decreases substantially from the value obtained in CH_3CN.

One rational is that the 1,7-hydrogen shift in S_1 is not a pure sigmatropic shift and may involve a charge buildup in the transition state (Scheme 2.6). This charge buildup

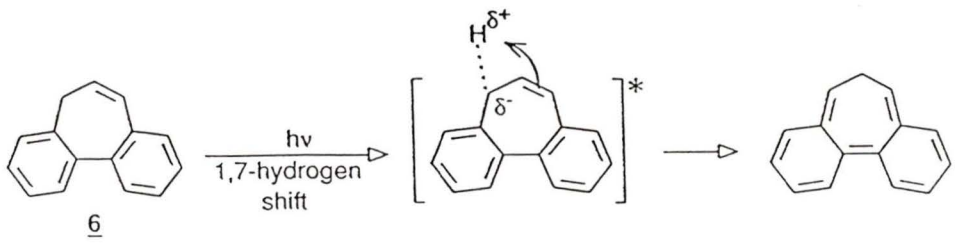

6

Scheme 2.6

could be important for DAC (**6**) since it may form a relatively stable carbanion in the excited state (*vide supra*). As well, Tezuka et. al.[47] proposed that the 1,7-hydrogen shift in S_1 of cycloheptatriene (**60**) may involve a polarized species.

This polarized species may be effected by the solvent if it exists for a relatively long period of time. A comparison of the quantum yields obtained for the 1,7-hydrogen shift of **6** and **34**[46] indicates that the latter molecule undergoes rearrangement much more efficiently. The decreased rate of rearrangement observed in DAC (**6**), results from the strain introduced into the system by the addition of a second benzene ring. A similar decrease in the rate of rearrangement is observed for cycloheptatriene (**60**) (eq. 2.11)[44] when it is substituted with a benzene ring as in **34**. This

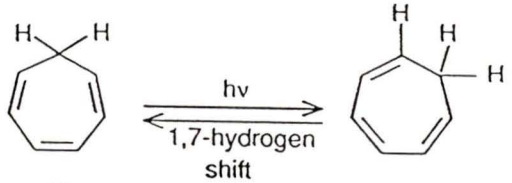

60 **(2.11)**

slower rate of rearrangement may lead to interaction between the solvent and the polarized species, proposed by Tezuka et. al.[47]. Solvents could therefore effect the 1,7-hydrogen shift of DAC (**6**) even though no solvent effects are observed for the similar rearrangement of **34** and **40**[46].

Photolysis of DAC (**6**) in C_6H_{12} should then only yield the di-π-methane product from T_1. By photolysing 6DDAC (**46**) in

C_6H_{12} it could be determined which mechanism operates in C_6H_{12}.

A similar photolysis of 6DDAC (**46**) in CH_3OD-CH_3CN would be useful in determining which formal di-π-methane rearrangement operates in CH_3OD. The quantum yield for rearrangement in this solvent is smaller then expected (*vide supra*). One can infer from the above discussion, that a more polar solvent should increase the efficiency of the 1,7-hydrogen shift. A more polar protic solvent, however, may prevent the 1,7-hydrogen shift by intercepting the proton involved in the shift. Accordingly an aprotic solvent more polar then CH_3CN should enhance the 1,7-hydrogen shift by not intercepting the proton involved in the shift.

2.3.4 Direct Irradiation of 6DDAC (46) in the Presence of H_2O

The procedure for direct irradiation of 6DDAC (**46**) was repeated in 70% H_2O-CH_3CN to determine the effect of H_2O on the formal di-π-methane rearrangement (eq. 2.12). The ^1H NMR (360 MHz) (Fig 2.6) indicated one photoproduct, **57**.

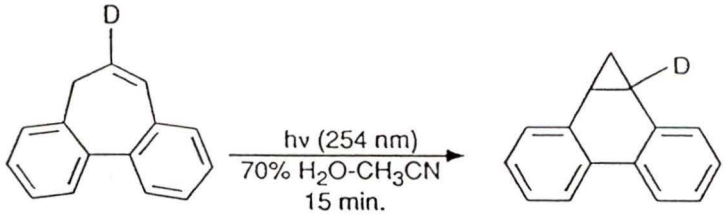

46 57 (2.12)

The product observed, **57**, results from the di-π-methane rearrangement in T_1. This indicates that H_2O acts as a quencher to deactivate the singlet excited state preventing

any singlet reactions such as the 1,7-hydrogen shift. The

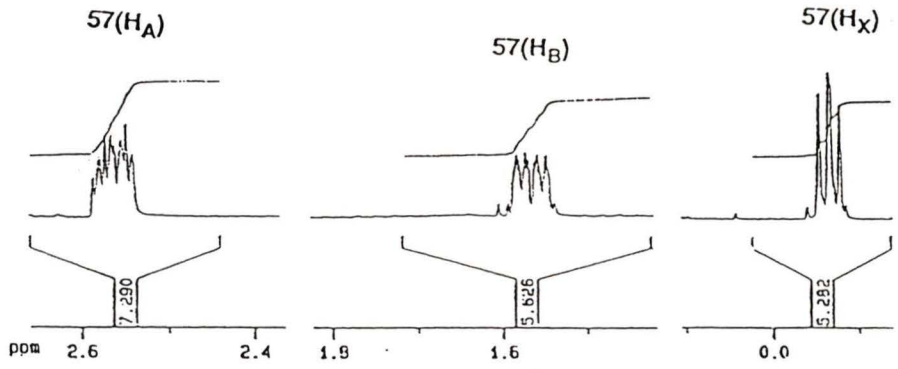

Figure 2.6 Regions of the ^{1}H NMR (from photolysis of 6DDAC (**46**) in 70% H_2O-CH_3CN) where H_A, H_B and H_X resonate.

proton exchange process is therefore more efficient than the 1,7-hydrogen shift of DAC (**6**). This can be understood when one considers the number of pathways, in Scheme 2.7 (*vide infra*), which deal with proton exchange. The quantum yield for exchange only accounts for the pathway leading to deuteration.

2.3.5 Proposed Scheme for the Photochemistry of DAC (6)

A complete picture of the deactivational processes of DAC (**6**) can now be drawn by combining all the results for the formal di-π-methane rearrangement and the proton exchange (Scheme 2.7). The relative efficiency of each deactivational pathway depends on the solvent conditions (*vide supra*).

The proton exchange mechanism involves D_2O, which is believed to deprotonate DAC (**6**) at position 5 to form a

carbanion **55**. D_2HO^+ then places the proton back on or rotates and places a deuterium at position 5. The proton exchange shown is an adiabatic photochemical process since the carbanion is formed in S_1 and is then transferred to the ground state. However the proton exchange could also occur via a diabatic photochemical process. As indicated for DAD (**1**) (*vide supra*) the diabatic process involves partial deprotonation in the excited state followed by deactivation to

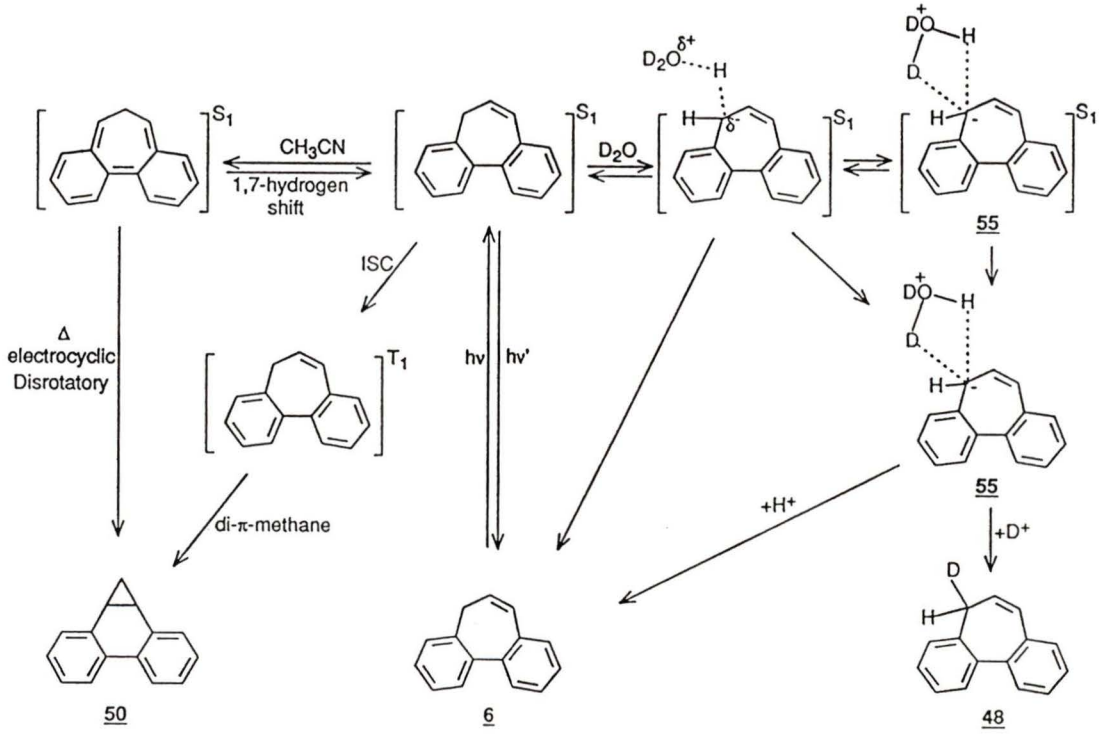

Scheme 2.7

the ground state. The proton exchange in Scheme 2.7 would represent a diabatic photochemical process if the carbanion **55** was removed from S_1.

The relative rates of the excited state proton exchange

of DAC (**6**) can be studied, indirectly, by fluorescence techniques. In the following section this aspect of the study of DAC (**6**) will be discussed.

2.4 Fluorescence Studies

Results presented (*vide supra*) indicate that the proton exchange process of DAC (**6**) involves the singlet excited state (S_1). Deactivation of aromatic molecules from S_1 predominately occurs by fluorescence[14]. The proton exchange process must compete with the fluorescence since it is also a pathway of deactivation from S_1. Many ESPT processes involving aromatic systems have been investigated utilizing correlation between proton exchange and fluorescence[48,49]. Fluorescence studies on DAC (**6**) should therefore provide indirect evidence clarifying the proton exchange process.

2.4.1 Fluorescence Quantum Yield

As indicated by the Jablonski diagram[9] (Fig. 2.7) several deactivational pathways exist for a molecule in S_1. In general deactivation from the lowest vibrational level of S_1 or T_1 occurs since molecules excited to higher levels undergo vibrational relaxation to return to the lowest excited state[14]. Deactivation of S_1 can occur by several pathways[9].

1) Fluorescence: Is the emission of light from the excited species resulting in deactivation ($h\nu'$).
2) Intersystem Crossing: Change in spin multiplicity

by crossing from the S_1 to T_1 state (ISC). Deactivation of T_1 can occur by phosphorescence (P) or by photochemical reactions.

3) Internal Conversion: This is vibrational relaxation between the electronic states S_3, S_2, S_1 (IC). It is less important between S_1 and S_0 since the energy gap here is larger then between higher energy states.

4) Photochemical Reactions: This includes reactions which lead to products, rearrangements of the excited species or quenching by transfer of energy to another molecule such as a solvent molecule (Sol).

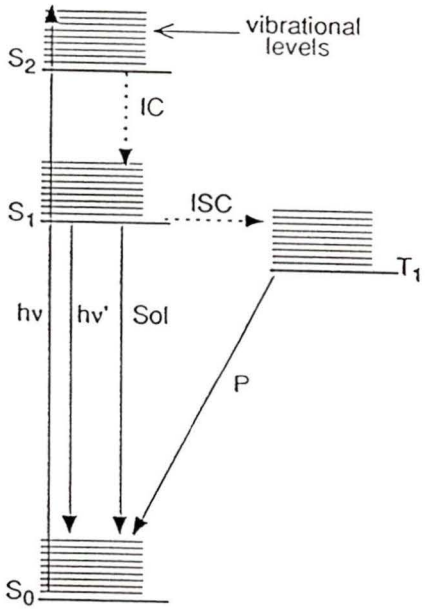

Figure 2.7 Jablonski diagram showing the pathways of deactivation from S_1.

A fluorescence quantum yield is a measure of that portion of the excited species which is deactivated by fluorescence[14].

The fluorescence quantum yield (Φ_f) of a compound can be obtained by comparing its fluorescence intensity with that of another compound, which has a known fluorescence quantum yield[50]. To make the comparison, both compounds must absorb the same number of photons[50] (*vide infra*). Another requirement is that the fluorescence bands of the two species must overlap[50]. This is required since a comparison of band areas is done to determine the unknown Φ_f (*vide infra*).

The standard chosen for DAC (**6**) was 2-aminopyridine (**61**). This standard has a fluorescence emission which overlaps that of DAC (**6**) (Fig. 2.8). Utilizing the procedure outlined in the Experimental, a Φ_f of 0.20 ± 0.06 was obtained in pure

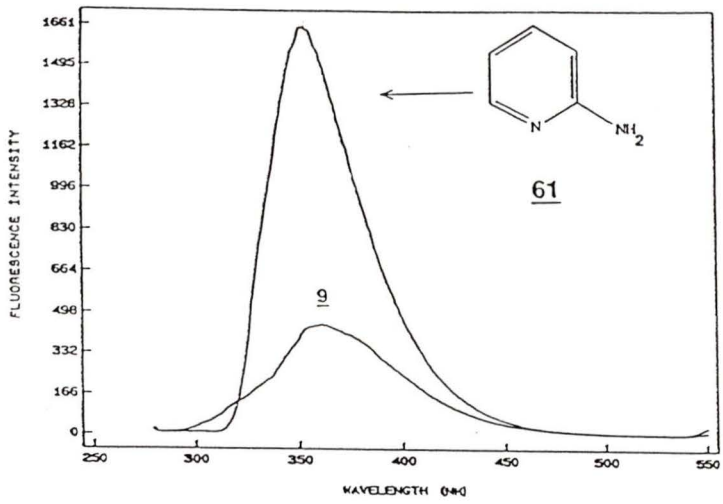

Figure 2.8 Overlap of the fluorescence emission spectra of 2-aminopyridine (**61**) and DAC (**6**) (λ_{ex} = 277 nm).

CH_3CN for DAC (**6**). This value indicates that ≈20% of excited DAC (**6**) is deactivated by fluorescence.

In the presence of water the fluorescence quantum yield drops dramatically (*vide infra*). This indicates that other deactivational processes, such as proton exchange, which occur when water is added, compete with fluorescence.

2.4.2 Fluorescence Lifetimes

The fluorescence lifetime (τ) of a molecule is the period of time required for its population in the excited state[9] to drop to 1/e. Several techniques exist for measurement of this quantity, which is on the order of nanoseconds. The technique utilized to obtain the fluorescence lifetime of DAC (**6**) was the single photon counting method[51]. This method involves the excitation of a sample with pulses of light. These pulses produce a fluorescence decay curve (Fig. 2.9). The fluorescence lifetime is then determined from this curve by a series of calculations. The method is termed single photon counting since the decay curve is constructed by measuring the time delay between a pulse and the arrival of a single photon[51].

Fluorescence lifetimes of DAC (**6**) were measured by E. Krogh[52] at the Center for Fast Kinetics Research (CFKR). Since that time a PTI LS-1 single photon counting device, capable of measuring nanosecond lifetimes, was made available at the University of Victoria. The fluorescence lifetimes measured

for DAC (**6**) in CH_3CN by E. Krogh[52] (4.0 ± 0.1 ns) and at the University of Victoria (3.9 ± 0.1 ns) are in good agreement.

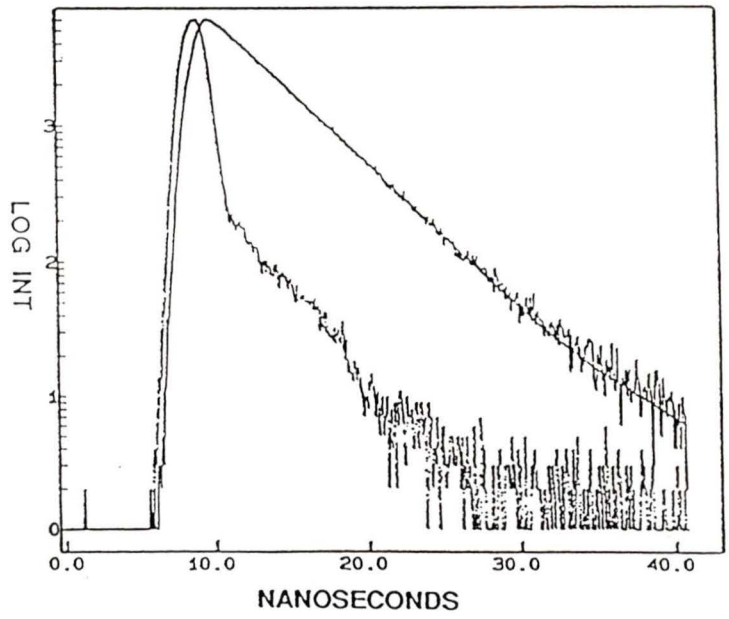

Figure 2.9 The upper curve shown is the fluorescence decay curve for DAC (**6**) in CH_3CN (λ_{ex}= 280 nm). The lower curve is the lamp profile.

The fluorescence lifetime of DAC (**6**) measured in pure CH_3CN is useful. Comparison of this lifetime with the lifetimes of other species, such a fluorene (**2**), indicates that the fluorescence lifetime is not a factor in determining whether or not a species will undergo proton exchange after excitation. If fluorene (**2**) had a lifetime much shorter than DAC (**6**), then one could reason that fluorene (**2**) is unreactive simply because insufficient time exists for the formation of a carbanionic intermediate. This in turn would indicate that the stability of the ICA, formed upon deprotonation in the

excited state, is not an important factor in determining the reactivity of the two species (*vide supra*). Fluorene (**2**), however, has a fluorescence lifetime of ≈6 ns in pure CH_3CN[3]. This is slightly greater then the fluorescence lifetime of DAC (**6**).

The above comparison should also be made in H_2O-CH_3CN, since this is the solution in which proton exchange occurs after excitation. In H_2O-CH_3CN the fluorescence lifetime of fluorene (**2**) remains unchanged[3]. The fluorescence lifetime of DAC (**6**) however is much shorter when H_2O is added[52]. This is expected as H_2O provides a more efficient pathway of deactivation (*vide infra*). Therefore the fluorescence lifetimes of DAC (**6**) and fluorene (**2**) do not determine which of the two will undergo proton exchange after excitation.

Another important use of the fluorescence lifetime obtained in pure CH_3CN, is that it can be utilized in the fluorescence quenching studies preformed in the following section.

2.4.3 Fluorescence Quenching Studies

The kinetics of the proton exchange observed for DAC (**6**) can be analyzed by fluorescence quenching studies. The quenching and exchange process are believed to be related for the following reasons.

Studies preformed on fluorene (**2**), DADA (**5**) and DAD (**1**) demonstrated that fluorescence quenching by H_2O only occurs if

proton exchange takes place. Fluorescence quenching by H_2O was not observed for either **2** or **5**. However, DAD (**1**) was quenched significantly.

Fluorescence quenching studies of DAD (**1**) and 5,5-dideuteriodibenzo[a,d]cycloheptene (**62**)[53] demonstrated a primary isotope effect[54] on the rate of quenching. The C-H bond, at the dibenzylic position, is therefore involved in the quenching process.

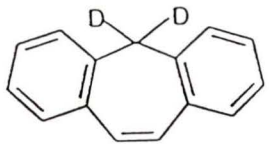

62

This correlation between proton exchange and fluorescence quenching is not unusual since the ESPT of numerous compounds have been investigated utilizing this correlation[48,49]. Fluorescence quenching studies on DAC (**6**) should therefore reveal information on the kinetics of the proton exchange process.

Rates for the excited state proton exchange process were determined from a Stern-Volmer plot. A Stern-Volmer plot is a graph of the ratio of fluorescence intensity without quencher (F_o) and with quencher (F) versus the concentration of quencher [Q] (Fig. 2.11)[51]. If a linear plot with an intercept of one is obtained then the rate of quenching (k_q) can be determined by substituting the slope, obtained from the plot, into the Stern-Volmer equation[51].

$$F_o/F = 1+k_q\tau_o[Q]$$

τ_o is the fluorescence lifetime (in the absence of quencher) of the compound being studied.

The fluorescence intensity of DAC (**6**) in the presence and absence of a quencher (H_2O) (Fig. 2.10) were obtained on a Perkin Elmer MPF-66 fluorescence spectrophotometer. The ratio F_o/F was then calculated from the fluorescence intensities and plotted against the concentration of H_2O (Table 2.7 and Fig. 2.11).

A linear plot was obtained with an intercept of one. Substitution of the slope obtained from the plot of DAC (**6**) in the Stern-Volmer equation, with τ_o = 4.0 ± 0.1 ns, provided a k_q of $(2.1\pm0.5)\times10^8$ $M^{-1}s^{-1}$. This value is similar to the one obtained for DAD (**1**) (k_q = $(1.6\pm0.5)\times10^8$ $M^{-1}s^{-1}$)[53].

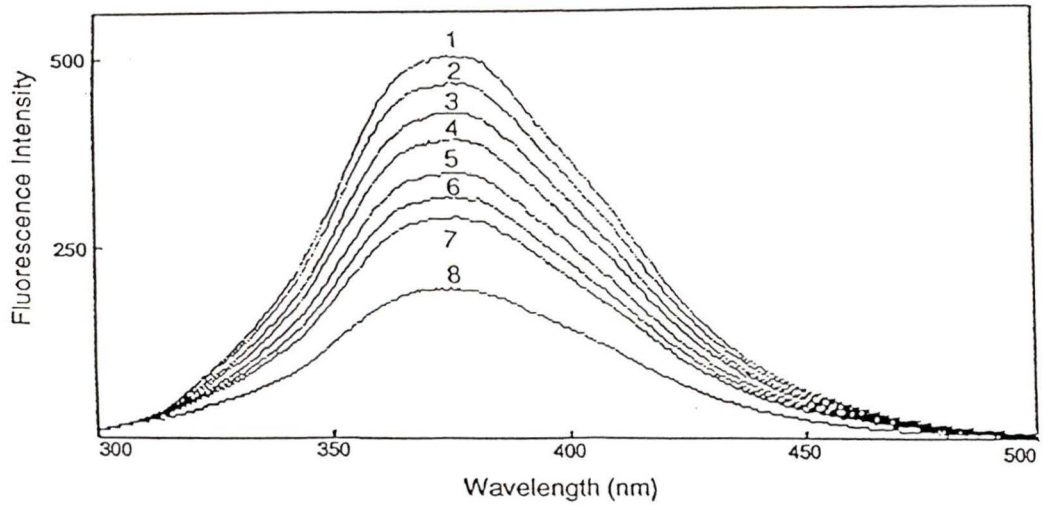

Figure 2.10 Fluorescence emission spectra of DAC (**6**) with various concentrations of H_2O in CH_3CN (1-8, shown in Table 2.7) (λ_{ex} = 260 nm).

Table 2.7 Data utilized to obtain the Stern-Volmer plot of DAC (**6**) with H_2O as the quencher.

#	$[H_2O]$(mol/L)	F_o/F
1	0	1.00±0.02
2	0.093	1.07±0.02
3	0.185	1.17±0.03
4	0.370	1.27±0.03
5	0.555	1.44±0.03
6	0.740	1.59±0.04
7	0.925	1.73±0.05
8	1.850	2.54±0.09

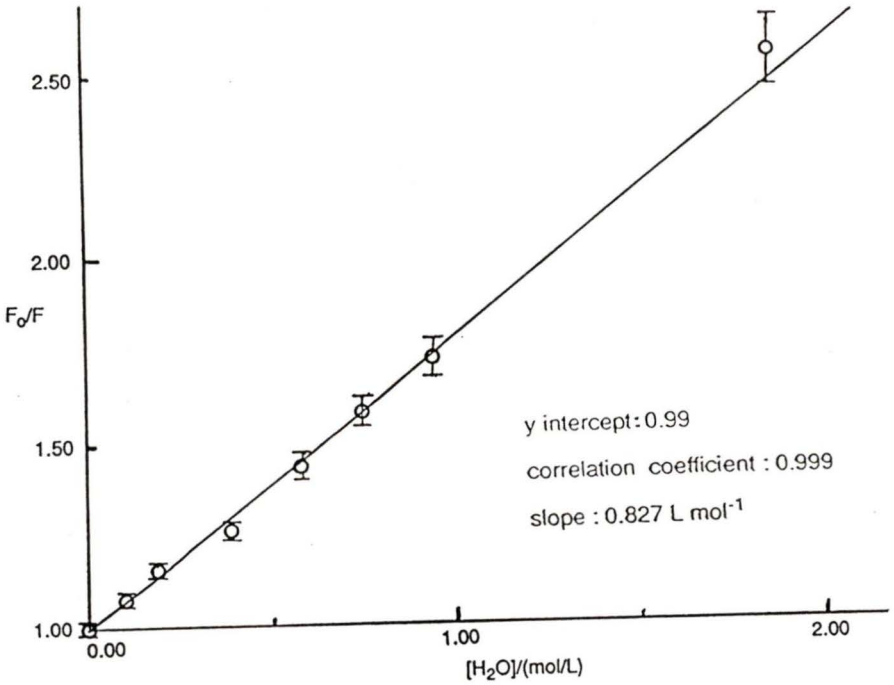

Figure 2.11 Linear Stern-Volmer plot for quenching of DAC (**6**) by H_2O.

This value can be related to the rate of deprotonation of DAC (**6**) in the excited state. k_q is a measure of the rate of deactivation from S_1 to the ground state surface. In Figures 1.7 and 1.8 it was demonstrated that deactivation of DAD (**1**) involved partial deprotonation (*vide supra*). k_q is therefore a measure of the rate of deprotonation of DAC (**6**) by H_2O.

2.4.4 Effect of pH on Fluorescence Quenching of DAC (6)

Another aspect of fluorescence quenching which can be useful for studying the proton exchange process of DAC (**6**) is the effect of pH. As indicated, the fluorescence quenching of DAC (**6**) involves the C-H bond at position 5 (*vide supra*). Therefore a change in pH, should effect the rate of quenching. As the pH is decreased, the rate of deprotonation will decrease. The rate of deprotonation is related to the rate of fluorescence quenching (*vide supra*). A change in the fluorescence quenching can therefore be related to the excited state pK_a of DAC (**6**).

Changes in the fluorescence quenching of aromatic compounds with changes in pH, are known to occur[55]. Under acidic conditions, an increase in fluorescence quenching is normally observed. This quenching process involves the protonation of aromatic species, such as naphthalene (**63**) (eq. 2.13). DAC (**6**) should therefore exhibit a reverse effect under acidic conditions, since fluorescence quenching of **6** involves deprotonation.

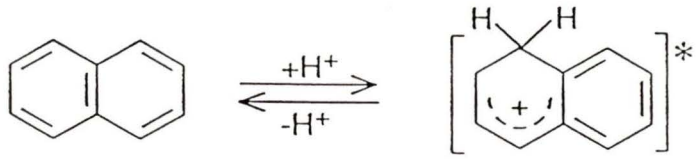

63 (2.13)

The effect of pH on the fluorescence quenching of DAC (**6**) was determined by measuring the fluorescence intensity of **6** in aqueous solutions of different pH or H_o (Table 2.8). The

Table 2.8 Fluorescence intensities of DAC (**6**) at various pH and H_o.

#	pH	Fluorescence Intensity *	#	H_o	Fluorescence Intensity *
1	14	27	8	0.04	151
2	13	94	9	-0.45	157
3	12	132	10	-1.18	230
4	10	109	11	-2.25	453
5	7	132	12	-3.3	556
6	2	143	13	-4.4	566
7	1	130			

* error of ±5 in fluorescence intensities

latter value, H_o, is a measure of the effective H^+ concentration below a pH of one[42]. The ratio F/F_o (where F_o is the maximum fluorescence intensity observed) was then calculated from the fluorescence intensities and plotted against pH and H_o to obtain the curve shown (Fig. 2.12).

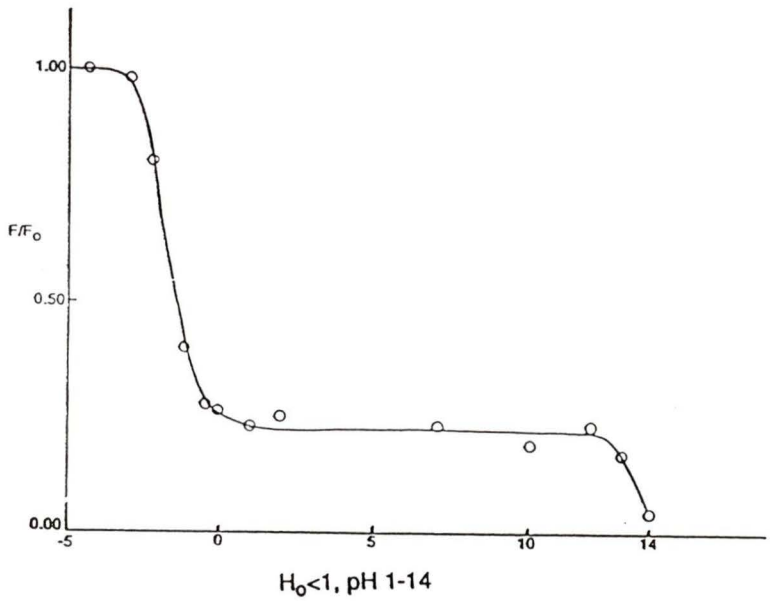

Figure 2.12 Plot of F/F_o vs pH and H_o for DAC (**9**).

Below H_o = 0 one can see a decrease in quenching or increase in fluorescence intensity. Interpretation of this curve is difficult, as the acid used in this region (H_2SO_4) could react with DAC (**6**)[21]. Aromatic systems do undergo electrophilic substitution to give sulfonic acids (eq. 2.14)[21].

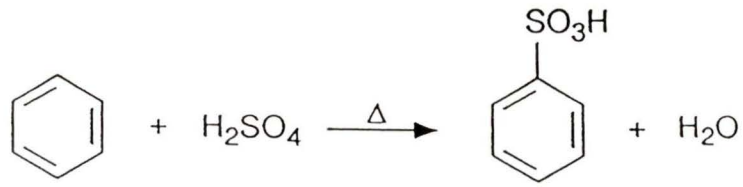

(**2.14**)

12

Similar effects would, however, be expected for naphthalene (**63**) but only an increase in fluorescence quenching is observed in this system[55]. The initial upward curve observed for DAC (**6**) can therefore be used to determine an upper limit

for the excited state acidity of DAC (**6**) (H_o<-2). This result indicates that a substantial change in the pK_a of DAC (**6**) occurs, when it is excited in the presence of H_2O (≈30 orders of magnitude).

2.5 Summary

DAC (**6**) exhibits photochemistry similar to that observed in the closely related systems, DAD (**1**) and 1,2-benzotropilidene (**34**). Like DAD (**1**), it undergoes an excited state proton transfer when photolysed in D_2O. The positions of the benzene rings of DAC (**6**) also allow for a 1,7-hydrogen shift, similar to that observed for **34**. Unlike **34**, isomerization cannot occur in DAC (**6**) and so deactivation of T_1 occurs by a true di-π-methane rearrangement. The relative rates of these photochemical processes are determined by the solvent utilized in the photolysis.

In aprotic solvents, only the rearrangement processes are observed. On addition of a protic solvent, a decrease in the amount of rearrangement takes place. This results from deactivation of the singlet state by the proton exchange process (carbon acid behaviour). The 1,7-hydrogen shift, which normally occurs in the singlet state in organic solvents, is not observed in the presence of H_2O. However, the true di-π-methane rearrangement, which is via T_1, is still observed in protic solvents.

Fluorescence quenching studies indicated a rate for the

photochemical deprotonation of DAC (**6**) of 2.1×10^8 $M^{-1}s^{-1}$. Similar studies in aqueous solutions of different pH and H_o, indicated that the ground state pK_a of DAC (**6**) changes by ≈30 orders of magnitude after excitation.

The deprotonation of DAC (**6**) may occur via a diabatic or adiabatic photochemical process. Either process involves the formation of a formally ground state antiaromatic 8π ICA. Other systems not capable of forming this type of array, such as fluorene (**2**) and DADA (**5**), do not undergo proton exchange after excitation. These results suggest that antiaromatic species are more readily formed from the excited state. Additional studies are required to delineate the mechanistic details of ionizing excited state carbon acids as well as their generality

CHAPTER THREE

EXPERIMENTAL

3.1 Instrumentation

Gas chromatography (GC) was carried out on a Varian 3700 gas chromatograph with a SE-54 capillary column in conjunction with a Hewlett-Packard 3390A integrator. Preparative HPLC was performed on a Waters model 500A prep. LC with a silica gel column. Mass spectra (MS) were recorded on a Perkin-Elmer Hitachi RMU-7 mass spectrometer and GC/MS on a Finnigan 3300 gas chromatography mass spectrometer using methane as a carrier gas and for ionization. UV spectra were obtained on a Pye Unicam SP8-400 or Perkin-Elmer Lambda 4B spectrometer. ^{1}H NMR spectra were recorded on either a Perkin-Elmer R32 (90 MHz) or Bruker WM250 (250 MHz) or Bruker AM360 (360 MHz) spectrometer using $CDCl_3$ as the deuterated solvent. Tetramethylsilane (TMS) was used as an internal standard in the 90 MHz instrument. ^{13}C NMR spectra were recorded on the Bruker WM250 (250 MHz) spectrometer using $CDCl_3$ as the solvent and standard. Fluorescence quenching studies were performed on a Perkin-Elmer MPF-66 fluorescence spectrometer. Fluorescence quantum yields and fluorescence lifetimes were measured on a PTI LS-1 spectrometer capable of both steady state fluorescence studies and single photon counting. Preparative photolysis were performed in a Rayonet RPR 100 photochemical reactor with 100 mL quartz tubes unless stated otherwise. Quantum yields were measured on a optical bench

utilizing an Oriel 200W Hg arc lamp and an Applied physics monochromator set at 280nm with 5nm slits. UV and small scale photolysis were performed in Suprasil quartz cuvettes.

3.2 Solvents and Reagents

All solvents were used without purification except CH_2Cl_2 which was distilled before use. Spectrophotometric grade acetone (Aldrich), acetonitrile (Fisher Chemicals) and pentane (Caledon) were used in GC, fluorescence studies and preparative HPLC, respectively. D_2O (MSD) used in the exchange studies had a purity of 99.9% and the CH_3OD (Aldrich) had a purity of 99.5%. Buffer solutions (Fisher Chemicals) were used for the pH solutions (1,2,7,10,12,13,14) in the fluorescence studies. Solutions with values of H_o (0.04,-0.45,-1.18,-2.25) were prepared using varying concentrations of H_2SO_4 (Fisher Chemicals). Lower values of H_o were achieved by using solutions of 50 and 60% by volume of concentrated H_2SO_4.

Other reagents such as diphenic anhydride, $NaBH_4$, $NaBD_4$ and PBr_3 were obtained from Aldrich and were utilized without purification.

3.3 Synthesis

3.3.1 Dibenzo[a,c]cyclohepta-6-one (42): Ketone **42** was prepared by the procedure of Tolbert and Ali[34] from diphenic anhydride (**41**). The crude brown material obtained was

purified by a bulb-to-bulb distillation using a Kugelrohr apparatus. A white crystalline solid (5 g) was obtained. The ^1H NMR (90 MHz) recorded agreed with the literature spectrum.

3.3.2 Dibenzo[a,c]cyclohepta-6-ol (43): The ketone **42** (4 g) was mixed with CH_3OH (100 mL) and cooled in an ice bath. A solution of $NaBH_4$ (1.5 g) in H_2O (20 mL) was then added via a dropping funnel over a 10 minute period along with a drop of NaOH (1 M). The resulting mixture was then heated to 45°C for 15 minutes then left to return to room temperature. It was then added to a cooled saturated solution of NH_4Cl in H_2O and mixed in a separatory funnel. Extraction of the alcohol **43** was done with two 100 mL portions of CH_2Cl_2. The organic extracts were combined and washed with an $NaCl-H_2O$ solution and dried over $MgSO_4$. Filtration of the $MgSO_4$ and evaporation of the organic solvents gave a thick brown oil (3.93 g, 97%) which crystallized under vacuum. This material was carried through to the next step without further purification as the ^1H NMR (90 MHz) obtained indicated few impurities; δ 1.5-2.2 ppm (broad, 1H,OH), 2.3-3.0(m, 4H, $-CH_2-$), 4.5 (t, J=6 Hz, 1H), 7.2-7.5 (m, 8H, arom.).

3.3.3 5*H*-Dibenzo[a,c]cycloheptene DAC (6): Alcohol **43** was dissolved in toluene (200 mL) and 80% H_3PO_4 (50 mL). A Dean-Stark trap was then connected and the mixture refluxed. H_2O formed from the dehydration after an hour was let out of the

trap and refluxing continued overnight. The resulting mixture was poured onto ice and left to warm up to room temperature. The organic layer formed was collected and the aqueous layer extracted with two 100 mL portions of hexanes. All organic layers were combined and washed with a saturated $NaCO_3H$-H_2O solution. $MgSO_4$ was then used to dry the organic solvent which was then filtered and evaporated to achieve a crude brown oil. Purification by a bulb-to-bulb distillation gave a colourless oil consisting of DAC (**6**) by ^1H NMR (250 MHz); δ: 3.0 ppm (d, J=7 Hz, 2H), 6.2 (dt, J=11, 7 Hz, 1H), 6.6 (d, J=11 Hz, 1H), 7.1-7.8 (m, 8H, arom.); MS (CI) m/z: 193 (M+1), 221 (M+29).

3.3.4 6-Deuteriodibenzo[a,c]cyclohepta-6-ol (44): Synthesis of the deuterated alcohol **44** was performed utilizing the same procedure followed in the synthesis of **43** only $NaBD_4$ was used. The scale of the reaction was cut to one quarter of the above reaction since only 1 g of the ketone **42** was used. Again no purification of the alcohol **44** produced (0.9 g, 89%) was performed as the $_1H$ NMR (90 MHz) indicated few impurities; δ: 1.5-2.2 ppm (broad, 1H, OH), 2.3-3.0 (m, 4H), 7.2-7.6 (m, 8H, arom.).

3.3.5 6-Deuterio-6-bromodibenzo[a,c]cycloheptane (45): The deuterated alcohol **44** (0.9 g) was dissolved in $CHCl_3$ (100 mL). PBr_3 (1.3 equiv.) was added while stirring the reaction

mixture which was then refluxed for 5 hrs. The resulting mixture was then cooled and poured into H_2O and the organic layer separated. The aqueous layer was extracted twice with 100 mL portions of CH_2Cl_2. These organic extracts were combined with the $CHCl_3$ removed earlier and washed with a saturated NaCl aqueous solution and then dried over $MgSO_4$. Filtration of the $MgSO_4$ and evaporation of the organic solvent gave a thick dark brown oil. This crude product was carried into the next step without purification since the ^1H NMR (90 MHz) indicated few impurities; δ: 2.7-3.5 ppm (m, 4H), 7.2-7.8 (m, 8H, arom.).

3.3.6 6-Deuterio-5*H*-dibenzo[a,c]cycloheptene (6DDAC) (46): Compound **45** was dissolved in a 3 M KOH-CH_3OH solution (50 mL) and refluxed for 1 hr. The resulting mixture was then poured into cold H_2O and extracted twice with 100 mL portions of CH_2Cl_2. The organic extracts were combined and dried over $MgSO_4$. Filtration of the $MgSO_4$ and evaporation of the organic solvent produced 1.8 g of a brown oil. Analysis by GC and ^1H NMR (90 MHz) indicated only 60% of the oil was 6DDAC (**46**). A preparative HPLC (Waters model 500A prep. LC) was therefore ran using pentane as the eluant on a silica gel column. A yield of 0.5 g was obtained consisting of 90% **46** by GC and ^1H NMR (360 MHz); δ: 2.9-3.2 ppm (broad, 2H), 6.65 (s, 1H), 7.2-7.8 (m, 8H, arom.); MS (CI) m/z: 194 (M+1), 222 (M+29).

3.4 Direct Photolysis (General Procedure)

Direct photolysis were performed by dissolving samples (40-100 mg) in CH_3CN. H_2O and D_2O if required were then added while stirring the CH_3CN solution. The resulting mixture was poured into a 100 mL quartz tube, cooled with a cold finger (≈17°C) and purged with 99.9% argon for 15-30 minutes. Both purging and cooling were continued during photolysis in a Rayonet RPR 100 photochemical reactor (254 nm lamps). The length of the photolysis varied from 5-30 minutes depending on the efficiency of the photochemical reaction.

Workup of the photolysis performed in CH_3CN was accomplished by simply evaporating off the organic solvent. Photolysis performed with H_2O or D_2O present were worked up by adding a saturated aqueous solution of NaCl. Two 100 mL portions of CH_2Cl_2 were then used to extract the organic materials. The organic extracts were then combined and dried over $MgSO_4$. Filtration of the $MgSO_4$ and evaporation of the organic solvent provided the photoproducts for analysis by GC, ^1H NMR and GC/MS.

3.4.1 DAC (6) in 50% D_2O-CH_3CN

Photolysis of DAC (**6**) (70 mg) in 50% D_2O-CH_3CN for 30 minutes resulted in four products according to GC/MS (CI) (isotemp 200°C); 6.93 min. (**6**:17%, **48**:23%, **49**:13%), 7.23 min. (**51**:7%), 8.13 min. (**50**:40%). The third peak due to DBN (**50**) also showed deuterium incorporation of 37%. Percent deuterium

incorporations were determined by subtracting the natural abundance of D and ^{13}C obtained from the MS of the starting material.

Analysis of the product mixture by ^{1}H NMR confirmed the total deuterium incorporation seen for **48** and **49** and the presence of DBN (**50**).

3.4.2 DAC (6) in CH_3CN

A shorter photolysis of DAC (**6**) (70 mg) in CH_3CN for 20 minutes gave two photoproducts by ^{1}H NMR (360 MHz). Yields were measured from the integration to give: **50** (67%), **51** (15%).

3.4.3 DAC (6) in CD_3CN

This photolysis follows the general procedure outlined for the quantum yield photolysis (*vide infra*). DAC (**6**) (0.01 mg) from a stock solution was photolysed in 10% CH_3CN-CD_3CN for 60 minutes in a suprasil quartz cuvette (3 mL) at a wavelength of 280 nm. According to GC/MS no deuterium incorporation occurred only rearrangement to give by GC (isotemp 180°C): 7.17 min. (**6**:92%), 7.36 min. (**51**:2%), 8.53 min. (**50**:6%).

3.4.4 Dark Reaction

A dark reaction was ran in 50% D_2O-CH_3CN, utilizing all the conditions utilized in the quantum yield photolysis (*vide*

infra) except the sample, DAC (**6**), was not irradiated. As well the dark reaction was allowed to sit for a longer period of time to insure that no reactions occurred. Analysis of the resulting mixture by GC, GC/MS and ^{1}H NMR (90 MHz) indicated no rearrangement and no proton exchange.

3.4.5 6DDAC (46) in CH_3CN

Both a 10 and 20 minute photolysis of 6DDAC (**46**) (40 mg) in CH_3CN were performed. Each photolysis gave the same ratio of photoproducts according to ^{1}H NMR (360 MHz): **48** (11%), **57** (35%), **58** (26%), **59** (27%).

3.4.6 6DDAC (46) in 70% H_2O–CH_3CN

Photolysis of 6DDAC (**46**) (40 mg) in 70% H_2O–CH_3CN for 15 minutes gave only one type of cyclopropyl product, **57** according to the ^{1}H NMR (360 MHz).

3.4.7 Triplet Quenching of 6DDAC (46) by O_2

The procedure for this photolysis was the same as that used in the photolysis of 6DDAC (**46**) in CH_3CN but instead of purging the system with argon O_2 was bubbled through. Two types of deuterated cyclopropyl products were visible according to the ^{1}H NMR (360 MHz): **58** (47%), **59** (53%).

3.5 Triplet Sensitization (General Procedure)

To insure that the quantities of sensitizer and sample were such that only the sensitizer absorbed at the wavelength of irradiation (350 nm), a UV of the two materials was taken, with the ratios to be used in the photolysis. DAC (**6**) was cut off at 310nm while the sensitizer 2-benzoylbenzoic acid (**56**) had an absorbance of 0.15 at 350 nm. The sample with a large excess of **56** was dissolved in the solvent mixture to be used. This mixture was then poured into a 100 mL pyrex tube and cooled to ≈17°C by a cold finger. Argon (99.9%) was then used to purge the system for 15-30 minutes before photolysis. Purging and cooling were both continued during the photolysis in a Rayonet RPR 100 photochemical reactor with 350 nm lamps. Photolysis times ranged from 10-60 minutes. The sensitizer **56** was removed after photolysis by washing the photoproducts with an 0.1M NaOH aqueous solution (150 mL) four times. The resulting organic layer was washed once with distilled H_2O and then dried over $MgSO_4$. Filtration and evaporation of the organic solvent was then done to obtain the photoproducts for GC, ^1H NMR and GC/MS analysis.

3.5.1 DAC (6) in CH_3CN

DAC (**6**) (10 mg) in 10 mL of CH_3CN was added to **56** (700 mg) in 90 mL of CH_3CN. This mixture was then photolysed for 10 minutes to give one product by GC (isotemp 200°C): 7.33 min. (**6**:87%), 8.52 min. (**50**:13%).

3.5.2 DAC (6) in D_2O–CH_3CN

DAC (**6**) (10 mg) and **56** (700 mg) were dissolved in CH_3CN (50 mL) and D_2O (50 mL) added with stirring. Triplet sensitization of the resulting mixture for 30 minutes resulted in only rearrangement by GC/MS (isotemp 200°C): 7.34 min. (**6**:26%), 8.54 min. (**50**:74%). No deuterium incorporation was observed.

3.5.3 6DDAC (46) in CH_3CN

Triplet sensitization of 6DDAC (**46**) (40 mg) with **56** (1.5 g) in CH_3CN for 60 minutes gave only one type of cyclopropyl product **57** by ^1H NMR (360 MHz).

3.6 Quantum Yields

Quantum yields were obtained on an optical bench using an Oriel 200W Hg arc lamp and an Applied physics monochromator set for 280 nm with slits of 5 nm. Samples were prepared by taking 0.300 mL of a 2.14×10^{-3} M stock solution and diluting it to 3.000 mL with the appropriate solvent mixture in suprasil quartz cuvettes. The UV absorbance of each sample was obtained at 280 nm to determine what percent of the light would be absorbed by the sample on the optical bench. The samples were then purged with argon (99.9% purity) prior to the photolysis (10-30 min.). Purging was continued during the photolysis to stir the solutions. No cold finger was utilized

since the intensity of the light source was not sufficient to heat up the samples appreciably. Photolysis times varied between 5-60 minutes depending on the conversion expected for the photoproducts. The yields of these photoproducts were kept low (<20%) to avoid secondary photoproducts.

Samples photolysed in organic solvents (CH_3CN, C_6H_{12}, CH_3OD) were simply worked up by evaporating off the solvent. Samples photolysed in the presence of D_2O or H_2O were placed in a 10 mL test tube and NaCl added to saturate the aqueous layer. Extractions with 3 portions of CH_2Cl_2 (3mL each) were then performed utilizing a pasteur pipette to mix the layers. The organic extracts were collected and dried over $MgSO_4$. Filtration and evaporation of the organic solvents provided the photoproducts required for analysis. These photoproducts were then dissolved in acetone (spec. grade) and GC analysis with GC/MS, if required, were preformed. Three GC injections were performed to achieve an average for the percent conversion to products resulting from the rearrangements (**50, 51**). The percent deuterium incorporations were determined from the GC/MS and the natural abundances of D and ^{13}C were again subtracted. The above procedure was performed two to three times for each solvent mixture to obtain more accurate quantum yield.

The light intensity in Einsteins/min/3 mL was measured before each photolysis with a chemical actinometer[41]. If the photolysis took longer then an hour the light intensity was

measured before and after the photolysis and an average taken. The chemical actinometer utilized was potassium ferrioxalate (PF) ($K_3Fe(C_2O_4)_3$)[40,41]. A solution of 0.0060M PF in 0.05M H_2SO_4 (250 mL) was prepared in the dark along with a 0.2% by weight solution of 1,10-phenanthroline (**64**) in distilled H_2O (to be used later). PF (3 mL) in a suprasil quartz cuvette was then photolysed on the optical bench in the dark for 5 minutes with argon purging to mimic the conditions used for photolysis of the samples. Along side the photolysed PF was placed another 3mL sample of PF, also in a suprasil quartz cuvette, to act as a blank.

Irradiation of PF leads to reduction of the Fe (eq. 3.1)[40]. The quantity of Fe^{2+} produced was measured by

$$2Fe^{3+} + C_2O_4^{2-} \longrightarrow 2Fe^{2+} + 2CO_2 \qquad \textbf{(3.1)}$$

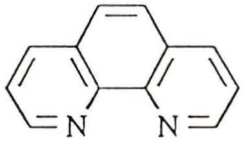

64

reacting it with 1,10-phenanthroline (**64**) to produce a complex. This complex absorbs at 510 nm. The quantity of Fe^{2+} can therefore be determine from the strength of this absorption.

The Fe^{2+} 1,10-phenanthroline complex was prepared by mixing 2.00mL of the 1,10-phenanthroline stock solution in a

10 mL volumetric flask with a buffer ($NaOAc \cdot 3H_2O$), 0.50 mL. A portion of the photolysed PF (1.00 mL) was then added to the volumetric and distilled H_2O added to make the solution up to the mark. Aluminium foil was wrapped around the volumetric which was then shaken vigorously and stored for 30 minutes in the dark to allow the complex to form. The above procedure was performed under a red light source and was repeated for the blank. A portion of the complex samples were then transferred to UV cuvettes and the absorption at 510 nm measured. The difference in absorptions (ΔA) of the photolysed PF and the blank PF was determined and substituted in the following equation for light intensity (I)[40] in Einsteins/min/3mL.

$$I = \frac{\Delta A \, v_2 \, v_3 \times 10^{-3}}{\epsilon \, \phi_\lambda \, t \, v_1}$$

Where:

v_1 is the vol. of irradiated actinometer withdrawn (1.00 mL).

v_2 is the vol. of actinometer irradiated (3.00 mL).

v_3 is the vol. of the volumetric flask (10.00 mL).

ε is the extinction coefficient for the Fe^{2+} 1,10-phenanthroline complex at 510nm ($1.11 \times 10^4 Lmol^{-1}cm^{-1}$).

ϕ_λ is the known quantum yield for Fe^{2+} formation at the wavelength used for photolysis, 280 nm (1.25)

t is the time of photolysis (5 min.)

The measured light intensity was then corrected to take into account only that percentage of the light absorbed by the samples. This corrected value along with the moles of photoproduct obtained in the photolysis of the DAC (**6**) were then substituted in the following equation to find the quantum yields (Φ). Two types of quantum yield were determined for DAC (**6**). Φ_{ex} is the quantum yield for the proton exchange process and Φ_{cycl} the quantum yield for cyclization or rearrangement both for DAC (**6**).

3.6.1 Φ_{cycl} of DAC (6) in CH_3CN

DAC (**6**) (6.44×10^{-7}mol) was photolysed on the optical bench in CH_3CN (3 mL) for 5 minutes. The sample used for photolysis was prepared by using 0.300 mL of the DAC (**6**) stock solution indicated at the start of this section. Three samples were prepared and photolysed however only two gave reasonable results (Table 3.1). The light intensity (I) measured was 2.81×10^{-7}Einsteins/min/3ml. Using an average of the values in

Table 3.1 Data from the photolysis of DAC (**6**) in CH_3CN for calculation of Φ_{cycl}.

sample #	% conv. to **50,51**	Int. Abs.	Φ_{cycl}
1	15.2	0.632	0.091
2	14.9	0.746	0.083

Table 3.1 a value for Φ_{cycl} of 0.087±0.004[56] was determined for DAC (**6**) in CH_3CN.

3.6.2 Φ_{cycl} of DAC (6) in C_6H_{12}

A stock solution of DAC (**6**) in C_6H_{12} (2.1 mM) was prepared and 0.300 mL ($6.44x10^{-7}$mol) of it mixed with 2.700 mL of C_6H_{12} in a cuvette and photolysed for 15 minutes. The resulting photoproducts were analyzed by GC (180-230°C, 2°C/min.) to obtain the following conversions (Table 3.2). The light intensity measured prior to the three photolysis was $2.90x10^{-7}$Einsteins/min/3mL. From the above data an average value for Φ_{cycl} of 0.015±0.001 was obtained for DAC (**6**) in C_6H_{12}.

Table 3.2 Data from the photolysis of DAC (**6**) in C_6H_{12} for calculation of Φ_{cycl}.

sample #	% conv. to **50,51**	Int. Abs.	Φ_{cycl}
1	8.9	0.848	0.015
2	9.9	0.908	0.016
3	9.0	0.911	0.015

3.6.3 Φ_{cycl} of DAC (6) in 70% H_2O-CH_3CN

Only two samples were photolysed in this determination of Φ_{cycl}. DAC (**6**) ($6.44x10^{-7}$mol) was photolysed in a 70% H_2O-CH_3CN solution for 10 minutes. UV analysis of the samples prior to photolysis and GC analysis (180-200°C, 2°C/min) after

photolysis gave the following data (Table 3.3). The value of I obtained before photolysis was 2.78×10^{-7}Einsteins/min/3mL. In 70% H_2O-CH_3CN DAC (**6**) has a value for Φ_{cycl} of 0.009±0.001.

Table 3.3 Data from the photolysis of DAC (**6**) in 70% H_2O-CH_3CN for the calculation of Φ_{cycl}.

sample #	% conv. to **50,51**	Int. Abs.	Φ_{cycl}
1	3.5	0.772	0.010
2	3.3	0.771	0.009

3.6.4 Φ_{cycl} and Φ_{ex} of DAC (6) in 70% CH_3OD-CH_3CN

A series of photolysis were preformed in this solvent mixture. Both Φ_{cycl} and Φ_{ex} were measured by photolysing DAC (**6**) (6.44×10^{-7}mol) in 70% CH_3OD-CH_3CN for varying lengths of time. UV analysis prior to photolysis and GC analysis (180-250°C, 5°C/min) after photolysis of the sample resulted in the following data (Table 3.4). For samples 1-3 I was 2.83×10^{-7} Einsteins/min/3mL and for samples 4-6 it was 2.92×10^{-7} Einsteins/min/3mL. These results indicate a decrease in Φ_{cycl} for longer photolysis.

In contrast GC/MS analysis gave the following results for Φ_{ex} (Table 3.5). Note the same values of I were used for each sample. The percent D incorporation are for DAC (**6**) therefore the moles converted to DBN (**50**) and **51** are subtracted when considering the number of moles of 5DDAC (**48**) produced. The

average deuterium incorporation of sample 1-3 is given in

Table 3.4 Data from the photolysis of DAC (**6**) in 70% CH_3OD-CH_3CN for the calculation of Φ_{cycl}.

sample #	Photolysis time (min.)	% conv. to **50,51**	Int. Abs.	Φ_{cycl}
1	10	2.4	0.626	0.007
2	15	3.3	0.606	0.007
3	20	3.9	0.602	0.006
4	40	5.0	0.668	0.004
5	50	5.0	0.667	0.003
6	60	5.1	0.676	0.002

Table 3.5 Data from the photolysis of DAC (**6**) in 70% CH_3OD-CH_3CN for the calculation of Φ_{ex}.

sample #	photolysis time (min.)	%D incorp.	Int. Abs.	Φ_{ex}
1-3	-	5	-	0.007
4	40	12	0.668	0.007
5	50	10*	0.667	0.005
6	60	16	0.676	0.007

*Value ignored due to large discrepancies in the MS.

Table 3.5 since only low inaccurate deuterium incorporation was observed in the shorter photolysis. Sample 5 was not reliable since large discrepancies existed in the GC/MS of

this sample. The average value of Φ_{ex} for DAC (**6**) in 70% CH_3OD-CH_3CN was 0.007±0.001. No average value for Φ_{cycl} could be obtained however the results for the shortest photolysis (0.007) should be the most accurate since there are fewer errors involved in short photolysis.

3.6.5 Φ_{ex} and Φ_{cycl} of DAC (6) in 70% D_2O-CH_3CN

Three samples of DAC (**6**) ($6.44x10^{-7}$mol each) were prepared in 70% D_2O-CH_3CN and each was photolysed for 10 minutes. Analysis by GC (180-234°C, 3°C/min) after photolysis and analysis by UV prior to it gave the following data for rearrangement (Table 3.6). The value of I obtained was $3.15x10^{-7}$Einsteins/min/3mL. An average value for Φ_{cycl} obtained from this data was 0.012±0.001.

Table 3.6 Data from the photolysis of DAC (**6**) in 70% D_2O-CH_3CN for the calculation of Φ_{cycl}.

sample #	%Conv. to **50,51**	Int. Abs.	Φ_{cycl}
1	4.4	0.682	0.011
2	5.0	0.677	0.013
3	4.4	0.690	0.011

GC/MS gave the data required for calculating Φ_{ex} (Table 3.7). Using the same value of I indicated above for the determination of Φ_{cycl} and the data in Table 3.7 a value for Φ_{ex}

of 0.034±0.006 was obtained.

Table 3.7 Data from the photolysis of DAC (**6**) in 70% D_2O-CH_3CN for the calculation of Φ_{ex}.

sample #	%D incorp.	Int. Abs.	Φ_{ex}
1	14	0.682	0.034
2	14	0.677	0.034
3	14	0.690	0.034

3.7 Fluorescence Quantum Yield Φ_f

Fluorescence quantum yields are a measure of the fraction of an excited species which is deactivated by fluorescence[16]. This quantity of DAC (**6**), was determined by using a standard, 2-aminopyridine (**61**), with a known fluorescence quantum yield[49]. This particular standard was chosen since the region it fluoresces in overlaps the region in which DAC (**6**) fluoresces (Fig. 2.8). Overlap of the fluorescence bands is required to insure that the energy of light being emitted is the same for both the standard and the sample[50].

Dilute solutions of each were prepared, DAC (**6**) in CH_3CN and **61** in 0.05 M H_2SO_4. Dilute solutions were used to prevent self quenching which can occur at high concentrations[51]. Samples of each were then placed in four sided suprasil quartz cuvettes and a UV spectrum recorded for each on the Pye Unicam SP8-400 to obtain a crossing point in the two spectra. The

absorbance of the sample and standard must be the same to insure that each absorbs the same number of photons[50]. Dilution of the DAC (**6**) solution was then performed to obtain two crossing points (280 nm and 282 nm).

The wavelengths at which the spectra crossed were found to be different on the PTi LS-1. This was determined by comparing the increases and decreases seen in fluorescence intensity with increases and decreases observed in the absorbance spectrum of **61**. If there is an increase in the absorbance there should also be an increase in the fluorescence intensity, since more light is being absorbed by the sample. By doing this comparison it was found that the PTi LS-1 differed by ≈-3.5 nm from the UV instrument. The excitation wavelengths chosen to determine Φ_f were therefore 276-277 nm instead of 280 nm and 278-279 nm instead of 280 nm.

The samples from the UV study were then purged with argon and placed in the fluoremeter. Excitation of each compound was done at the wavelengths indicated above and the resulting fluorescence spectra recorded. The areas in each fluorescence spectra were then measured and substituted in the following equation[50] to determine Φ_f for DAC (**6**).

$$\Phi^u = \Phi^n \frac{\phi^u}{\phi^n} \left(\frac{\eta^u}{\eta^n}\right)^2$$

Where:

ϕ^u and ϕ^n are the areas under the sample and standard

fluorescence curves respectively.

Φ^u and Φ^n are the fluorescence quantum yields for the sample and standard (0.60±0.05)[41] respectively.

η^u and η^n are the refractive indexes of the solvent used with the sample (CH_3CN:1.3)[41] and that used with the standard (0.05M H_2SO_4:1.33)[57].

Using all the areas obtained, at the four different excitation wavelengths, several values of Φ^u were calculated (Table 3.8). An average of these values was then taken to achieve the value of 0.20±0.06.

Table 3.8 Fluorescence quantum yields (Φ_f) obtained for DAC (**6**) at four different excitation wavelengths.

λ_{ex} (nm)	ϕ^u/ϕ^n	Φ^u
276	0.388	0.24
277	0.334	0.20
278	0.294	0.18
279	0.240	0.15

3.8 Fluorescence Lifetime Of DAC (6) in CH_3CN

The fluorescence lifetime of DAC (**6**) in CH_3CN was measured by utilizing the single photon counting method[51] (*vide supra*). This method is very sensitive therefore very pure samples must be used to avoid interference from impurities. Fluorescing impurities can interfere by producing an abnormal

biexponential fluorescence decay curve. Also due to the methods sensitivity, very dilute samples were used to reduce the possibility of self quenching[50]. A dilute sample of DAC (**6**) in CH_3CN (dried over 4Å molecular sieves) was prepared in a four sided suprasil quartz cuvette. The sample was purged extensively with argon since O_2 can effect the fluorescence lifetime[51]. A lifetime of 3.9±0.1 ns was obtained for DAC (**6**) by exciting at 280 nm and monitoring the emission at 360 nm.

3.9 Fluorescence Quenching Studies of DAC (6) With H_2O

Quenching studies were preformed on a Perkin-Elmer MPF-66 fluorescence spectrophotometer using H_2O as the quencher. A dilute sample ($\approx 10^{-5}$M) of DAC (**6**) in CH_3CN was prepared and its fluorescence spectrum recorded. Dilute solutions are required to prevent self quenching[51], as indicated in the other fluorescence studies. Several tests were performed to insure that the fluorescence observed was due only to DAC (**6**). The purity of the DAC (**6**) sample was determined by recording its excitation spectrum. If the sample was pure then the excitation spectrum should resemble the absorbance spectrum[14]. A resemblance was observed in the present case. The purity of the solvents used, was determined by looking for extraneous fluorescence in the absence of DAC (**6**). No fluorescence was observed in the distilled H_2O or CH_3CN (dried over 4Å molecular sieves) used in the experiment. The photostability of the sample over time was determined by monitoring the samples

fluorescence intensity for ≈1 hour. Little variation in the fluorescence intensity of DAC (**6**) was observed. The effect of O_2 on the fluorescence of DAC (**6**) was also determined by obtaining a fluorescence spectra in the presence and absence of O_2. No difference was observed between the two spectra, indicating that O_2 does not quench the S_1 state of DAC (**6**).

Fluorescence quenching studies are based on a comparison between the fluorescence intensities of samples, with varying quantities of quencher. The concentration of the species being quenched and all instrumental parameters therefore must be kept constant to measure the effect of the added quencher. The excitation wavelength used was 260 nm with slits of 5nm. A series of samples were prepared with varying concentrations of H_2O in CH_3CN (<2 M). Three samples were prepared at each concentration of H_2O. The fluorescence intensity was measured for each and an average of the three values taken. The values of fluorescence intensities over the range of H_2O concentrations (Table 2.7) were then used to obtain the Stern-Volmer plot (Fig. 2.11) shown in the previous chapter (2.4.3).

3.10 Effect of pH on Fluorescence Quenching of DAC (6)

The aforementioned procedure was also used in this study, however, the dilute stock solution of DAC (**6**) was prepared in EtOH (95%). As well an excitation wavelength of 230 nm was used with 4 nm slits. Samples with different pH (1, 2, 7, 10, 12, 13, 14) and H_o (0.04, -0.45, -1.18, -2.25, -3.3, -4.4)

values were prepared in 10% EtOH(95%)/H_2O. The fluorescence intensities, of DAC (**6**), were measured at different pH or H_o. The data obtained (Table 2.8) was then used to obtain the plot (Fig. 2.12) shown in the previous chapter (2.4.4).

REFERENCES

1. Fratev, F.; Monev, V.; Janoshek, R. *Tetrahedron* **1982**, *38*, 2929.

2. Padma, E. J.; Jug, K. *Tetrahedron* **1986**, *42*, 417.

3. Wan, P.; Krogh, E.; Chak, B. *J. Am. Chem. Soc.* **1988**, *110*, 4073.

4. *Comprehensive Carbanion Chemistry;* Buncel, E., Durst, T., Eds; Elsevier: Amsterdam, 1984; Part A.

5. Limits estimated from the pk_a of cycloheptatriene (**60**) and 5*H*-dibenzo[a,d]cycloheptane (**5**) from ref 6.

6. Weber, K. *Z. Elektrochem.* **1931**, *815*, 18.

7. FÖrster, Th. *Z. Elektrochem.* **1950**, *54*, 42.

8. Weller, A. *Z. Elecktrochem.* **1952**, *56*, 662.

9. Wayne, R. P. *Principles and Applications of Photochemistry;* Oxford University Press: Oxford, 1988.

10. Weller, A. *Prog. React. Kinet.* **1961**, *1*, 189.

11. Ireland, J. F.; Wyatt, P. A. H. *Adv. Phys. Org. Chem.* **1976**, *12*, 131.

12. Kelly, R. N.; Schulmann, S. G. *Molecular Luminescence Spectroscopy: Methods and Applications-Part II;* Wiley: New York, 1988.

13. Vander Donckt, E. *Prog. React. Kinet.* **1970**, *5*, 273.

14. Turro, N. J. *Modern Molecular Photochemistry;* Benjamin/Cummings: Menlo Park, 1978.

15. Bernasconi, C. F.; Terrier, F. *J. Am. Chem. Soc.* **1987**, *109*, 7115.

16. Mason, S. F.; Smith, B. E. *J. Chem. Soc. (A)* **1969**, 325.

17. Kresge, A. J. *Acc. Chem. Res.* **1975**, *8*, 354.

18. The curves shown are drawn to demonstrate how an adiabatic and diabatic process would occur and are not based on experimental results.

19. Zimmerman, H. E. *Acc. Chem. Res.* **1971**, *4*, 272.

20. Breslow, R. *Acc. Chem. Res.* **1973**, *6*, 393.

21. Ege, S. N. *Organic Chemistry;* D. C. Heath and Co.: Toronto, 1984.

22. Scott, L. T.; Jones, Jr., M. *Chem. Rev.* **1972**, *72*, 181.

23. Bally T.; Masamune, S. *Tetrahedron* **1980**, *36*, 343.

24. Lloyd, D. *Non-Benzenoid Conjugated Carbocyclic Compounds;* Elsevier: Amsterdam, 1984.

25. Streitwieser, Jr., A. *Molecular Orbital Theory for Organic Chemists;* Wiley: New York, 1961.

26. Cundall, R. B.; Robinson, D. A.; Pereira, L. C. *Advances in Photochemistry* **1977**, *10*, 147.

27. McAuley, I.; Krogh, E.; Wan, P. *J. Am. Chem. Soc.* **1988**, *110*, 600.

28. Hixson, S. S.; Mariano, P. S.; Zimmermann, H. E. *Chem. Rev.* **1973**, *73*, 531.

29. Pomerantz, M.; Gruber, G. W. *J. Am. Chem. Soc.* **1971**, *93*, 6615.

30. a) Zimmermann, H. E.; Grunewald, G. L. *J. Am. Chem. Soc.* **1966**, *88*, 183. b) Zimmermann, H. E.; Binkley, B. W.; Givens, R. S.; Sherwin, M. A. *ibid.* **1967**, *89*, 3932. c) Zimmermann, H. E.; Binkley, B. W.; Givens, R. S.; Grunewald, G. L.; Sherwin, M. A. *ibid.* **1969**, *91*, 3316.

31. Zimmermann, H. E.; Pratt, A. C. *J. Am. Chem. Soc.* **1970**, *92*, 6267.

32. Morrison, H. *Organic Photochemistry;* Padwa, A., Ed.; Marcel Dekker, Inc.: New York, 1979; vol. 4.

33. Burdett, K. A.; Shenton, F. L.; Yates, D. H.; Swenton, J. S. *Tetrahedron* **1974**, *30*, 2057.

34. Tolbert L. M.; Ali, M. Z. *J. Org. Chem.* **1982**, *47*, 4793.

35. Banciu, M.; Thuy, P. L.; Elian, M.; Draghici, C.; Cioranescu, E. *Rev. Rou. Chim.* **1981**, *26*, 115.

36. Kotera, K.; Motomura, M.; Miyuzuki, S.; Okada, T.; Matsukauia, Y. *Tetrahedron* **1968**, *24*, 1727.

37. Clar, E.; McAndrew, B. A.; Zander, M. *Tetrahedron* **1967**, *23*, 985.

38. MÜller, E.; Kessler, H.; Suhr, H. *Tetrahedron Lett.* **1965**, *8*, 423.

39. Richardson, D. B.; Durrett, L. R.; Martin, Jr., J. M.; Putnam, W. E.; Slaymaker, S. C.; Duoretzky, I. *J. Am. Chem. Soc.* **1965**, *87*, 2763.

40. Murov, S. L. *Handbook of Photochemistry;* Dekker: New York, 1973.

41. Kuhn, H. J.; Braslavsky, S. E.; Schmidt, R. *Pure and Appl. Chem.* **1989**, *61*, 187.

42. Lowry, T. H.; Richardson, K. S. *Mechanism and Theory in Organic Chemistry 3rd ed.;* Harper and Row: New York, 1987, ch. 3.

43. Pavia, D. L.; Lampman, G. M.; Kriz, Jr., G. S. *Introduction to Spectroscopy: A Guide for Students of Organic Chemistry;* Sanders College: Philadelphia, 1979.

44. Ter Borg, A. P.; Kloosterziel, H. *Rec. Trav. Chim.* **1965**, *84*, 241.

45. Carey, F. A.; Sundberg, R. J. *Advanced Organic Chemistry: Part A: Structure and Mechanisms 2nd ed.;* Plenum Press: New York, 1984.

46. Wan, P. Shukla, D. unpublished results.

47. Tezuka, T.; Kikuchi, O.; Houk, K. N.; Puddon-Row, M. N.; Santiago, C. M.; Rondan, N. G.; Williams, Jr., J. C.; Gandour, R. W. *J. Am. Chem. Soc.* **1981**, *103*, 1367.

48. Shizuka, H.; Tobita, S. *J. Am. Chem. Soc.* **1982**, *104*, 6919.

49. a) Stryer, L. *J. Am. Chem. Soc.* **1966**, *88*, 5708. b) Tsutsumi, K.; Shizukz, H. *Chem. Phys. Lett.* **1977**, *52*, 485. c) Shizuka, H. *Acc. Chem. Res.* **1985**, *18*, 141.

50. Eaton, D. E. *Pure and Appl. Chem.* **1988**, *60*, 1107.

51. Lakowicz, J. R. *Principles of Fluorescence Spectroscopy;* Plenum Press: New York, 1983.

52. Wan, P.; Krogh, E. unpublished results.

53. Wan, P.; Budac, D. manuscript in preparation.

54. Maskill, H. *The Physical Basis of Organic Chemistry;* Oxford University Press: New York, 1985.

55. Stevens, C. G.; Strickler, S. J. *J. Am. Chem. Soc.* **1973**, *95*, 3922.

56. The errors obtained for the product quantum yields of cyclization and exchange were derived from the standard deviation in the tabulated values.

57. *Handbook of Chemistry and Physics 48th ed.;* Weast, R. C., Selby, S. M., Eds.; The Chemical Rubber Co.: Cleveland, 1967.

VITA

Surname: Budac Given Names: David Patrick

Place of Birth: Fort St. John, B.C. Date of Birth: Aug. 22/63

Educational Institutions Attended:

University of Victoria 1983-1990

Degrees Awarded:

B.Sc. (Honours) University of Victoria 1988

Publications:

1. Wan, P.; Budac, D.; Krogh, E. *J. Chem. Soc., Chem. Commun.* **1990**, 255.

2. Wan, P.; Budac, D.; Earle, M.; Shukla, D. *J. Am. Chem. Soc.* **1990**, *112*, 8048.

PARTIAL COPYRIGHT LICENSE

I hereby grant the right to lend my thesis to users of the University of Victoria Library, and to make single copies only for such users or in response to a request from the Library of any other university, or similar institution, on its behalf or for one of its users. I further agree that permission for extensive copying of this thesis for scholarly purposes may be granted by me or a member of the University designated by me. It is understood that copying or publication of this thesis for financial gain shall not be allowed without my written permission.

Title of Thesis: Photochemistry of 5*H*-Dibenzo[a,c]cycloheptene

Author [redacted]
(Signature)

DAVID PATRICK BUDAC
(Name in Block Letters)

Jan 10/91
(Date)